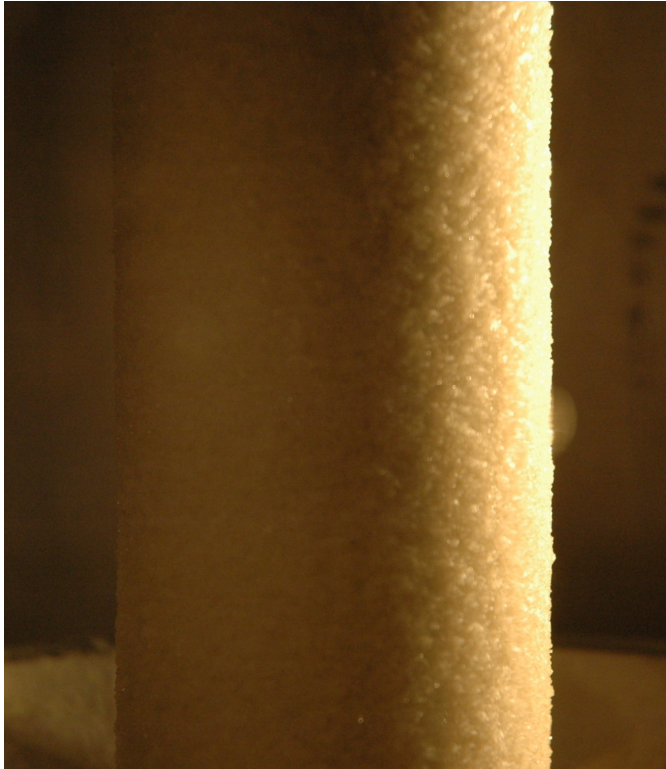


CHALMERS



Experimental investigation and modelling of sodium scale dissolution rates in black liquor evaporators

*Master's Thesis within the Innovative and Sustainable Chemical Engineering
programme*

ANNA BROBERG

ANDERS ÅKESJÖ

Department of Energy and Environment
Division of Heat and Power Technology
CHALMERS UNIVERSITY OF TECHNOLOGY
Göteborg, Sweden 2012

MASTER'S THESIS

Experimental investigation and modelling of sodium scale dissolution rates in black liquor evaporators

Master's Thesis within the *Innovative and Sustainable Chemical Engineering*
programme

ANNA BROBERG

ANDERS ÅKESJÖ

SUPERVISOR:

Erik Karlsson

EXAMINER

Mathias Gourdon

Department of Energy and Environment
Division of Heat and Power Technology
CHALMERS UNIVERSITY OF TECHNOLOGY

Göteborg, Sweden 2012

Experimental investigation and modelling of sodium scale dissolution rates in black liquor evaporators

Master's Thesis within the *Innovative and Sustainable Chemical Engineering* programme

ANNA BROBERG

ANDERS ÅKESJÖ

© ANNA BROBERG, ANDERS ÅKESJÖ

Department of Energy and Environment

Division of Heat and Power Technology

Chalmers University of Technology

SE-412 96 Göteborg

Sweden

Telephone: + 46 (0)31-772 1000

Cover:

A layer of sodium salt scaling covering an evaporator tube.

Chalmers Reproservice

Göteborg, Sweden 2012

Experimental investigation and modelling of sodium scale dissolution rates in black liquor evaporators

Master's Thesis in the *Innovative and Sustainable Chemical Engineering* programme

ANNA BROBERG

ANDERS ÅKESJÖ

Department of Energy and Environment

Division of Heat and Power Technology

Chalmers University of Technology

ABSTRACT

Few publications address how to efficiently remove sodium scales in black liquor evaporators. The lack of information makes the cleaning inefficient and subjective. In this work, the sodium scale dissolution rate has been experimentally investigated and a model for the dissolution process has been developed. The aim was to relate the dissolution rate to wetting degree and temperature of the wash liquid. The experiments were conducted in a pilot plant evaporator of the falling film type. A saline solution consisting of sodium carbonate and sodium sulphate was evaporated on the outside of a vertical stainless steel tube. The removal of the resulting scaling layer was then studied at different temperatures and wetting degrees.

An effective method for investigating the removal of sodium scales in falling film evaporators was developed and a model was constructed that successfully could predict the obtained experimental data. The washing behaviour proved to be strongly dependent on how the scales were distributed along the tube. It was confirmed that scales grow from the bottom of the tube and upwards until the layer reaches an equilibrium thickness. The dissolution rate was found to follow a 1st order expression with regards to the concentration difference between the scaling layer surface and the bulk of the wash liquid. The model was developed in the temperature interval 45-85 °C and wetting degrees of 0.13 kg/ms up to 0.44 kg/ms. Based upon the model, three correlations applicable to the industry were developed in order to estimate the saturation degree of the outgoing wash liquid.

Key words: Dissolution model, sodium sulphate, sodium carbonate, scaling, removal of sodium salts, evaporator cleaning, falling film

Experimentell undersökning och modellering av upplösningshastigheter för natriuminkrustering i svartlutsindunstare

Examensarbete inom masterprogrammet *Innovative and Sustainable Chemical Engineering*

ANNA BROBERG

ANDERS ÅKESJÖ

Institutionen för Energi och Miljö

Avdelningen för Värmeteknik och maskinlära

Chalmers tekniska högskola

SAMMANFATTNING

Få publikationer tar upp hur natriuminkrustering i svartlutsindunstare effektivt kan tas bort. Bristen på information gör tvättningen ineffektiv och subjektiv. I detta arbete har upplösningshastigheten för natriuminkrustering undersökts experimentellt och en modell som beskriver upplösningen har utvecklats. Målet var att relatera upplösningshastigheten till vätningsgrad och temperaturen på tvättvätskan. Experimenten utfördes i en fallfilmsindunstare i pilotskala. En saltlösning innehållande natriumkarbonat och natriumsulfat indunstades på utsidan av en vertikal tub gjord i rostfritt stål. Avlägsnandet av det bildade inkrusterlagret studerades vid olika temperaturer och vätningsgrader.

En effektiv metod för undersökningen av hur natriuminkrustering avlägsnas i fallfilmsindunstare utvecklades och en modell som framgångsrikt kunde förutsäga erhållen experimentell data togs fram. Tvättbeteendet visade sig vara starkt beroende av fördelningen av inkrustering på tuben. Vidare bekräftades det att inkrustering växer nerifrån och upp på tuben tills lagret når en jämviktstjocklek. Upplösningshastigheten visade sig följa ett första ordningens uttryck med avseende på skillnaden i koncentration mellan inkrusterlagrets yta och tvättvätskans bulk. Modellen utvecklades för temperaturintervallet 45-85 °C och för vätningsgrader mellan 0.13-0.44 kg/ms. Baserat på modellen utvecklades tre korrelationer som uppskattar mätnadsgraden hos den utgående tvättvätskan, något som kan vara mycket relevant för industrin.

Nyckelord: Upplösningsmodell, natriumsulfat, natriumkarbonat, inkrustering, avlägsnande av natriumsalter, tvättning av indunstare, fallfilm

Contents

ABSTRACT	I
SAMMANFATTNING	II
CONTENTS	III
PREFACE	V
NOTATIONS	VII
1 INTRODUCTION	1
1.1 Objective	2
1.2 Method	2
2 BACKGROUND	3
2.1 Kraft pulping	3
2.1.1 Black liquor	3
2.1.2 Evaporation of black liquor	4
2.2 Falling film theory	4
2.3 Crystallisation	5
2.4 Fouling in heat transfer equipment	7
2.4.1 Black liquor fouling	7
2.4.2 Sodium salt scaling	8
2.5 Foulant cleaning procedures in the pulp industry	10
2.6 Modelling of scale removal in other industries	11
3 EXPERIMENTAL SETUP AND WORK	15
3.1 Scaling layer build-up	15
3.1.1 The pilot plant	15
3.1.2 Operating conditions	17
3.2 Washing	19
3.2.1 Method	19
3.2.2 Parameters and limitations	21
4 DEVELOPMENT OF A SCALE DISSOLUTION RATE MODEL	23
4.1 Model suggestions	23
4.1.1 1 st order model	23
4.1.2 Diffusion-reaction model	24
4.2 Calculation methods	24
4.3 Scale distribution	25
5 EXPERIMENTAL RESULTS AND DISCUSSION	27
5.1 Washing behaviour	27

5.2	Dissolution of scales	28
5.3	Temperature and wettability dependence	29
5.4	Deviating washing behaviour	30
5.5	Relevance of wetting degree	31
5.6	Scale cracking	32
6	MODELLING RESULTS AND DISCUSSION	33
6.1	Evaluation	33
6.2	Parameter optimisation	35
6.3	Validity of the proposed dissolution model	38
7	MODEL IMPLEMENTATION	41
8	CONCLUSIONS	43
9	FURTHER RESEARCH	45
	REFERENCES	47
	APPENDIX	51
1.	Volume expansion factor	51
2.	Experimental data	53

Preface

In this study, the dissolution rate of burkeite and dicarbonate has been experimentally investigated. The experiments and following evaluation were carried out during January to May in 2012. The work is part of the master programme *Innovative and Sustainable Chemical Engineering* and resulted in this master thesis. The work was performed at the division of Heat and Power Technology within the department of Energy and Environment, Chalmers University of Technology, Sweden.

This master thesis has been executed with Dr. Mathias Gourdon as examiner and Ph.D student Erik Karlsson as supervisor. Thank you for your invaluable support and creative discussions during this thesis. A special thank you is directed to Prof. Lennart Vamling who shared his interesting theories and thoughts of the studied subject. Your input was highly valued. All experiments have been performed in a pilot plant evaporator at the division of Heat and Power Technology at Chalmers University of Technology. The pilot plant was built in cooperation of Metso Power AB and Chalmers University of Technology. Many thanks to Ulf Andersson, Metso Power AB, for the introduction and practice regarding the operation of the pilot plant. We are also most grateful for the help provided by Bengt Erichsen regarding maintenance and improvements of the pilot plant. None of the experiments could have been conducted without the assistance of Mathias Gourdon, Erik Karlsson, Viktor Andersson and Bengt Erichsen.

Finally, we will always remember the fun moments we shared with Mathias and Erik during this time.

Gothenburg, May 2012

Anna Broberg & Anders Åkesjö

Notations

Greek letters

θ	Delta function	$[-]$
δ_{bulk}	Thickness of the bulk	$[m]$
δ_d	Thickness of the diffusion boundary layer	$[m]$
δ_r	Thickness of the reaction boundary layer	$[m]$
δ_x	Thickness of the laminar boundary layer	$[m]$
Γ	Wetting degree	$[kg/ms]$
ΔA	Surface area of a discretized cell	$[m^2]$
Δt	Time step	$[s]$
μ	Dynamic viscosity	$[Pas]$
ν	Kinematic viscosity	$[m/s^2]$
ρ	Density	$[kg/m^3]$
τ	Shear stress	$[Pa]$

Roman letters

A	Surface area of the solid-liquid interface	$[m^2]$
c^*	Saturation concentration of the solution	$[kg_{salt}/kg_{solution}]$
c_b	Concentration in the bulk flow	$[kg_{salt}/kg_{solution}]$
c_d	Concentration at reaction-diffusion interface	$[kg_{salt}/kg_{solution}]$
c_i	Concentration at solid-liquid interface	$[kg_{salt}/kg_{solution}]$
c_{OH}	Hydroxyl ion concentration in the solvent	$[mol/m^3]$
c_s	Concentration at the solid surface	$[kg_{salt}/kg_{solution}]$
c_x	Concentration of contaminant to be removed	$[mol/m^3]$
d_{tube}	Outer diameter of the evaporator tube	$[m]$
D_{AB}	Diffusivity	$[m^2/s]$
g	Gravitational acceleration	$[m/s^2]$
k	Transport coefficient	$[kg_{solution}/m^2s]$
k_1	Rate constant	$[kg/s]$
k_d	Transport coefficient in the diffusion layer	$[kg_{solution}/m^2s]$
k_r	Reaction coefficient in the reaction layer	$[kg_{solution}/m^2s]$
L	Length of tube covered with scales	$[m]$
\dot{m}_{water}	Mass flow rate of water	$[kg/s]$
m_i	Mass of species i	$[kg]$
M	Mass of fouling layer	$[kg]$
M_0	Initial mass of fouling layer	$[kg]$
M_i	Molar weight of species i	$[g/mol]$
n	Reaction order	$[-]$
n_i	Moles of species i	$[-]$
r	Dissolution rate	$[kg_{salt}/m^2s]$
r_i	Dissolution rate for layer i	$[kg_{salt}/m^2s]$
Re	Reynolds number	$[-]$
s	Total film thickness	$[m]$
s_{avg}	Total average film thickness	$[m]$
s_{lam}	Total laminar film thickness	$[m]$
s_{turb}	Total turbulent film thickness	$[m]$

SD_{in}	Saturation degree of the ingoing wash liquid	[%]
SD_{out}	Saturation degree of the outgoing wash liquid	[%]
t	Time	[s]
t_0	Initial time	[s]
T	Temperature	[°C]
$T_{avg,in}$	Temperature ingoing wash liquid	[°C]
$T_{avg,out}$	Temperature outgoing wash liquid	[°C]
v_z	Flow velocity in z direction	[m/s]
x	Mole fraction $Na_2CO_3 / (Na_2SO_4 + Na_2CO_3)$	[mol/mol]
x_{scale}	Scaling layer thickness	[m]

1 Introduction

Most process industries rely on operations that involve heat transfer between two fluids in some sort of heat exchange equipment. Depending on the type of fluids, solid material tends to adhere more or less to the heat transferring surfaces and during operation a layer is built up on these surfaces. This contamination process is called fouling. Another term frequently used is scaling, which refer to hard, crystal-like fouling. Any type of fouling layer works as an insulation material and will reduce the heat transfer, making the heat transfer equipment inefficient. To compensate for the deterioration of heat transfer, additional fuel has to be put in. In many cases the fuel is fossil and an increase in the usage will have a significant impact on the environment. Thus it is important to have as high efficiency of the apparatus as possible to minimise the environmental impact.

The forest industry is of great importance in Sweden and stands for 10-12 % of all industry in Sweden when it comes to employment, export and sale (Skogsindustrierna 2010). Due to high availability of raw material and on-going pioneering research the Swedish wood based industries have flourished and been successful on the global market (Brännvall et al. 2008). Sweden are nowadays the second largest exporter of cellulose based products and exporting over 85 % of the pulp and paper production and about 70 % of the sawn timber (Skogsindustrierna 2010). However, the pulp and paper industry is a very energy-intensive line of business and great effort is continuously put into making the pulp mill self-sufficient of energy (Axelsson et al. 2006; Costa et al. 2007; Mateos-Espejel et al. 2010). A crucial part in achieving high energy-efficiency is the recovery boiler where waste chemicals and wooden residues are incinerated to produce steam on-site and to recover chemicals to the process. The possibility of improved internal integration of heat sources and heat sinks has also been investigated (Axelsson et al. 2006). Waste water reduction and insulation of process equipment are other methods to reduce the energy demand (Mateos-Espejel et al. 2010).

In a pulp mill, the cellulose fibres are liberated from the wood chips by digestion in cooking liquor. After digestion, the fibres are further refined in washing and bleaching stages. The wooden residues and the spent chemicals from the digestion are recovered as black liquor, which is incinerated in the recovery boiler to supply the pulp mill with energy. To increase the heat value of the fuel, the black liquor is first thickened in an evaporation plant (Gourdon 2009). During the evaporation of black liquor inorganic salts are precipitated and large amounts of crystals are formed. These crystals mainly consist of sodium salts (Frederick, Verrill, et al. 2004c). As the dry content of the black liquor increases there is a risk of fouling of the heat transferring surfaces. The two most important crystals in scaling of black liquor evaporators are burkeite and dicarbonate with the approximate compositions $2\text{Na}_2\text{SO}_4 \cdot \text{Na}_2\text{CO}_3$ and $\text{Na}_2\text{SO}_4 \cdot 2\text{Na}_2\text{CO}_3$ respectively (Gourdon et al. 2011). Scale formation on heat transferring surfaces will significantly reduce the transfer of heat between the heating medium, usually steam, and the black liquor. As a result, the performance of the evaporator will decrease together with the capacity. Since less water will be evaporated, the final dry content of the black liquor exiting the evaporation plant will also decrease. A lower dry content means a lower-value fuel with an inferior heating value compare to more concentrated black liquor (Clay 2008). If no actions are taken, the recovery boiler efficiency will decrease and the pulp mill will no longer be self-supplying in energy, making either the import of energy or a complete shutdown of the mill necessary. A

reduced heat transfer in the evaporator will thus have a negative effect both when it comes to environmental impact and profitability. In reality, the fouling should never be allowed to reach such a crucial level that complete shut-down of the pulp mill is the only option.

To prevent a reduced efficiency of the evaporator plant fouling needs to be minimised. There are several techniques available on the market that prevent fouling, but none is fully effective. Fouling will to some degree occur despite any precautions taken, hence removal of formed scales will be necessary. Today very little knowledge exists of how to remove scaling. Previous research has mainly focused on how to prevent fouling by optimising operating conditions rather than how to efficiently remove scales (Euhus et al. 2003; Haag & Stigson 2003; Frederick, Verrill, et al. 2004b; Verrill & Frederick 2005; Gourdon 2009). When the heat transfer is too low, the evaporator effect is simply stopped and cleaned for an arbitrary time (Müller-Steinhagen 1997) using water, acidic or alkaline solution (Gill & Henderson 1995). The lack of guidelines makes the cleaning process unreliable and subjective; the cleaning is usually scheduled on regular basis and has little or no relation to the degree of fouling (Schmidl & Frederick 1998). A more efficient washing can reduce the time needed for cleaning and reduce the use of wash liquid together with providing a reliable way to determine when the heat surfaces are considered clean. Consequently, there exists a need for a validated, trustworthy washing method to commonly be used by pulp mills.

1.1 Objective

The objective of this master thesis is to perform an experimental investigation of sodium salt dissolution rate and develop a model that can describe the dissolution process. The dissolution rate of a scaling layer formed on the outside of a tube will be studied under different operating conditions in a pilot plant. The washing conditions investigated are temperature and wetting degree. The goal is to produce a washing model that relates the rate of dissolution to the studied parameters.

1.2 Method

A pilot plant evaporator at the division of Heat and Power Technology at Chalmers was used to carry out experiments at a size relevant to the industry. The evaporator is of a falling film type. A layer of sodium scales was formed on the outside of a tube by evaporation of a solution of sodium carbonate and sodium sulphate. Subsequently, the scales were washed using deionised water as wash liquid. The effect of temperature and wetting degree was investigated in the experimental series.

Based on previous modelling found in literature of scale removal in other industries, a mathematical model was proposed. MATLAB was used to compare the model to experimental data and to evaluate the model accuracy.

2 Background

2.1 Kraft pulping

The most common pulping process in Sweden is the alkaline Kraft process (*Figure 2.1*) (Gourdon 2009), also called sulphate cooking. The aim of pulping is to liberate the fibres from the wood matrix by removing lignin, i.e. delignification. In the first stage wood chips are treated at elevated temperature in cooking chemicals, so-called white liquor, until a certain level of delignification has been reached. The cooking chemicals mainly consist of sodium hydroxide and sodium sulphide. The pulp fibres are then washed and bleached to finally be used in the production of paper or other cellulose products. The lignin-rich solution remaining after the washing step is called weak black liquor. To recycle the cooking chemicals the diluted black liquor is concentrated in evaporators and then burnt in a recovery boiler. The formed smelt is dissolved into green liquor that is transformed into white liquor in a causticising stage (Brännvall et al. 2008).

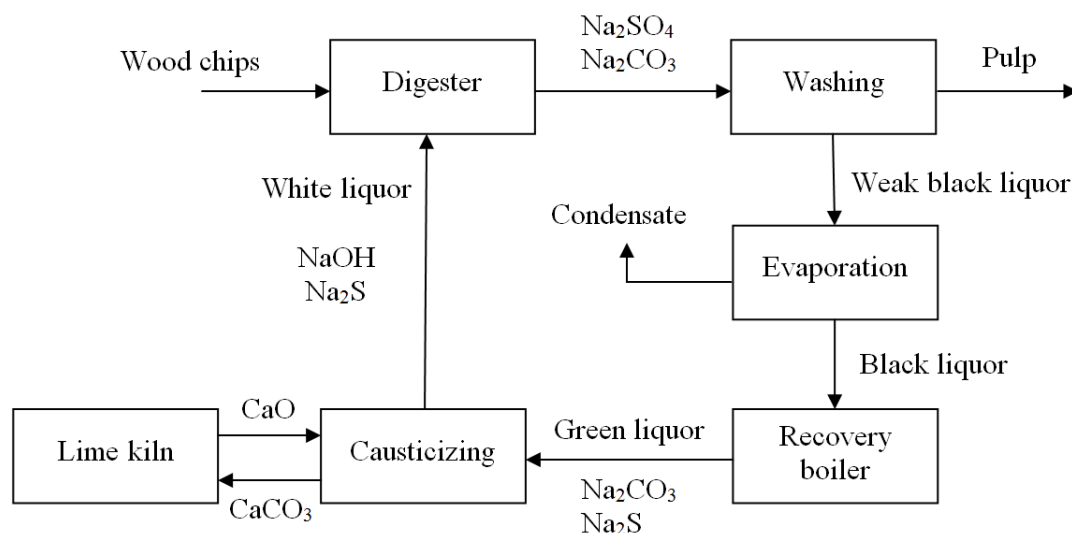


Figure 2.1 A simplified overview of the Kraft process.

The complex structure and its importance in the recovery cycle have made black liquor a popular research area. Besides optimising the evaporation process, the composition of black liquor is of interest and especially the use of lignin as raw material for speciality chemicals or gasification of black liquor.

2.1.1 Black liquor

Black liquor is a viscous, alkaline residue from the pulping process that contains several organic and inorganic compounds. Two thirds of the solids in black liquor are various organic compounds, predominately lignin (29-45 %) and extractives (25-35 %), and the remaining third is inorganic compounds originating from the cooking chemicals and the wood chips. The exact concentrations of the compounds depend on wood raw material and cooking conditions (Brännvall et al. 2008).

The different salts in the black liquor will affect the boiling point of the solution and cause a boiling point elevation. A boiling point elevation is a rise in boiling point between a pure solute and a solution when measured at the same pressure. It is caused by the addition of non-volatile species to the pure solute (Shi 2002).

The physical properties of black liquor will change with varying chemical composition and are therefore important to measure and continuously monitor during operation. The density can be used to monitor the amount of dissolved material in the liquor: a density close to water indicates a diluted liquor. Another important property is viscosity which will influence the flow conditions and thereby the heat transfer in the evaporator. When the dry solid content rises, viscosity increase and is strongly affected by both dry solid content and temperature (Gourdon 2009).

2.1.2 Evaporation of black liquor

Pulp mills nowadays strive towards being self-supplying of energy or even to have an excess of heat to distribute to neighbouring customers. The main way to meet the high energy demand of the pulp mill is with steam production in the recovery boiler where black liquor is used as fuel. To increase the heating value of the black liquor more than 90 % of the water in the weak black liquor is removed in an evaporation plant (Brännvall et al. 2008). Modern pulp mills use multi-effect evaporators to concentrate black liquor from 14-18 % to above 70 % (Chen & Gao 2004; Gourdon 2009). The steam formed in the first stage is used as heating medium in the second stage and so on, making the evaporation more energy efficient (Brännvall et al. 2008). Apart from having a counter-current flow of steam and black liquor, there are many different alternatives on the market with the aim to achieve higher energy efficiency.

During recent years, the use of falling film evaporators has increased and it is nowadays the standard type of equipment used for black liquor evaporation (Brännvall et al. 2008). One of its main advantages is the short contact time between the black liquor and the heat transfer surface resulting in less fouling of the surfaces. The black liquor enters at the top of the evaporator and a fast-falling, thin film coats the heat transfer surface, tubes or plates, due to gravitational forces. As the black liquor falls down it is partially evaporated (Chen & Gao 2004). In addition to water, methanol and other organic compounds with vapour pressures near that of water will also be partly evaporated (Brännvall et al. 2008).

2.2 Falling film theory

The falling film process will be dependent on the properties of the liquid, especially the flow behaviour. In a falling film evaporator the solvent will flow as a thin film over the scaling layer and the behaviour of the film will depend on whether it is in the turbulent or laminar flow region. As the film becomes more turbulent a boundary layer will form at the tube wall and the film will be divided into a laminar boundary layer and a turbulent bulk region with different velocity profiles. If the film is completely laminar the boundary layer will occupy the entire film and the overall velocity profile will be parabolic (*Figure 2.2*). A more turbulent film will enhance the mass transfer since the mixing of the bulk is improved. At the wall the no-slip condition will apply, i.e. the velocity at the wall is presumed to be zero.

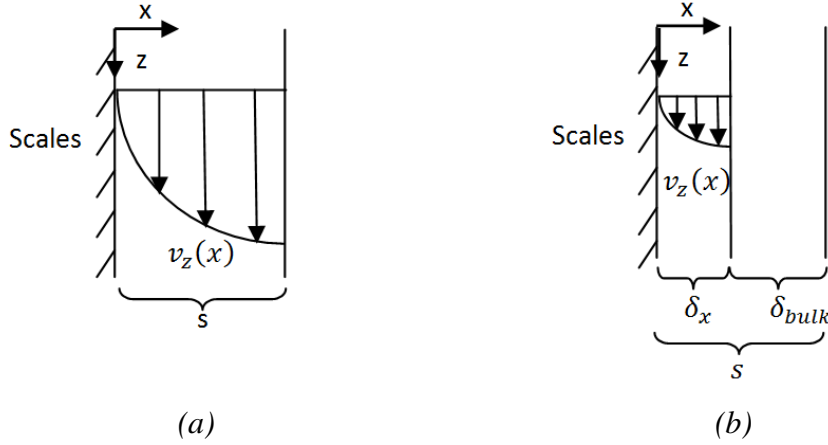


Figure 2.2 Flow profiles for (a) a completely laminar film and (b) a turbulent bulk flow with a laminar boundary layer.

Instead of flow rate, wetting degree can be used to define the rate of the falling film. The wetting degree Γ is in this study based on the mass flow rate of water and the outer perimeter of the tube (Equation 2.1). The use of wetting degree instead of flow rate makes the study more comparable to other falling film evaporators.

$$\Gamma = \frac{\dot{m}_{water}}{\pi d_{tube}} \quad (2.1)$$

To estimate which flow profile the film will have during washing the Reynolds number for the film flow can be calculated (Equation 2.2). For Reynolds numbers below 400 the film can be considered wavy laminar and at higher Reynolds numbers the film will pass into the turbulent region.

$$Re = \frac{\Gamma}{\mu} \quad (2.2)$$

The thickness of the liquid film covering the tube is dependent on whether the film is laminar or turbulent. Schnabel (1988) presented two correlations for calculating the film thickness based on the Reynolds number (Equation 2.3 and 2.4). The value 3 in equation 2.3 can be changed to 2.4 to account for waves and ripples that occur in non-ideal laminar films where the Reynolds number is near the interface between the two flow regions (Schnabel 1988).

$$s_{lam} = \left(\frac{3\nu^2}{g}\right)^{1/3} Re^{1/3} ; Re < 400 \quad (2.3)$$

$$s_{turb} = 0.302 \left(\frac{3\nu^2}{g}\right)^{1/3} Re^{8/15} ; Re > 400 \quad (2.4)$$

When using equations 2.3 and 2.4 care should be taken with respect to the definition of Reynolds number since they are only valid when the Reynolds number is calculated according to equation 2.2.

2.3 Crystallisation

The precipitation of solid crystals in a solution, i.e. crystallisation, is the essential mechanism for scaling of black liquor evaporators. As water is evaporated the solids

concentration in the black liquor rises and at a certain concentration salt crystals begin to precipitate (Gourdon 2009). The solubility of a substance is defined as a thermodynamic limit for how much salt that can be dissolved at equilibrium. The solubility is dependent on the type of solute and solvent and on temperature (Frederick, Shi, et al. 2004). During the course of evaporation the solubility limit for burkeite and dicarbonate will be exceeded and a degree of supersaturation will occur (Figure 2.3). Supersaturation is a measure of how much the solubility limit is surpassed and is a necessity for crystallisation to take place. Crystals will spontaneously start to form when the concentration of the solution exceeds yet another limit: the metastable limit. Supersaturation is not a stable thermodynamical state but it can be maintain as long as the concentration is within the metastable region (Verrill & Frederick 2005).

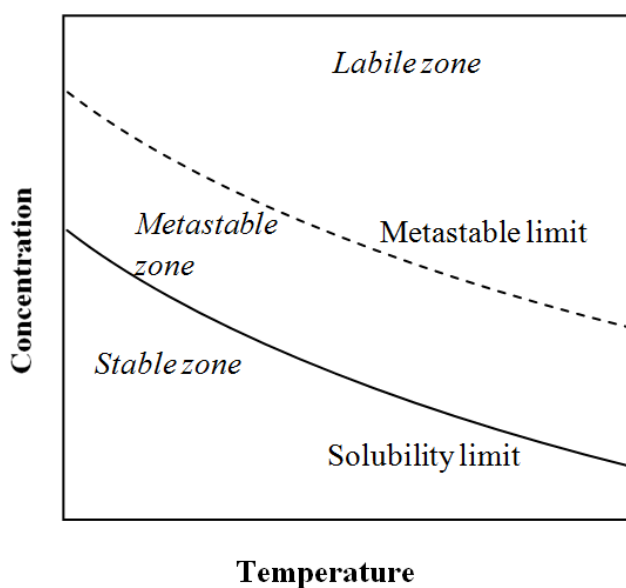


Figure 2.3 Solubility diagram for a system with inverse temperature dependence. As water is evaporated, the concentration will increase. No crystals will be formed in the stable region. When the solubility limit is exceeded the solution becomes supersaturated. In the metastable region crystals can form on already existing crystals but spontaneous nucleation is improbable. In the labile zone however, spontaneous nucleation is very likely to occur.

New crystals can form via either primary or secondary nucleation. Primary nucleation can occur spontaneously when the metastable limit is exceeded without the influence of already formed crystals in the solute. Primary nucleation rapidly generates large amounts of small crystals, usually resulting in a solute concentration decrease below the metastable limit (Frederick, Verrill, et al. 2004a). Secondary nucleation occurs in the presence of crystals in the solute and can occur through several mechanisms such as breeding or contact nucleation, i.e. collisions with equipment or other crystals (Shi 2002).

2.4 Fouling in heat transfer equipment

The precipitation of crystals causes severe problems in heat exchange equipment when the crystals adhere to the heat transfer surfaces. The phenomenon is called fouling and can consist of both soft coatings and hard crystals that adhere to the surfaces, the latter referred to as scaling. Crystals formed on the heat transfer surfaces will act as an insulation layer that can significantly reduce the heat transfer (Frederick, Shi, et al. 2004).

2.4.1 Black liquor fouling

Black liquor contains several inorganic substances (*Table 2.1*) that can form scales during evaporation (Shi 2002). The chemical composition of the black liquor determines to which degree scaling occurs in the evaporator and also what sort of scales that will be formed (Brännvall et al. 2008). When the black liquor reaches a dry solid content of approximately 50 % the concentration of sodium sulphate and sodium carbonate have exceeded the metastable limit and sodium scales start to form (Shi 2002).

Table 2.1 Content of dry solids for some inorganic compounds in weak black liquor (% wt). Adapted from Schmidl & Frederick (1998).

	Na	Na ₂ CO ₃	Na ₂ SO ₄	Na ₂ S	Ca (ppm)
Mean	18.4 %	10.0 %	6.03 %	0.79 %	409
Std dev	1.65 %	2.6 %	4.18 %	0.92 %	278

In addition to sodium scales, scaling can also be caused by calcium. Together with dissolved organic substances calcium forms complexes in the black liquor. These complexes decompose when subjected to high temperature and release calcium ions that bind to carbonate ions and crystallise on the heat transferring surfaces. The precipitation of calcium crystals is however a highly temperature-dependent process that can be controlled by thermal deactivation in which the black liquor is heated before entering the evaporator. The calcium carbonate crystals thus precipitate in the bulk and do not participate in any scaling of the heat transferring surfaces (Shi 2002). Other scaling species include aluminium silicates and calcium silicates (Gourdon 2009).

Besides several salts forming scales, black liquor contains other species that contributes to fouling. About 0.85 wt.% of the black liquor is residual soap (Schmidl & Frederick 1998). Soap is incorporated in the crystal lattice when different scales adhere to the heat transfer surfaces, giving an enhanced fouling rate. Moreover, soap contains dissolved calcium and fibres that contribute to fouling. Fibre is not a primary fouling agent but can accelerate other fouling mechanisms. Another fouling agent is lignin but the precipitation of lignin is highly dependent on the pH of the black liquor, hence easily controlled (Clay 2008). There are several ways to reduce fouling and one of the simpler ones is to have a high flow rate over the heat transfer surfaces of the black liquor.

2.4.2 Sodium salt scaling

The final dry content of the black liquor after evaporation has been increased by the pulp mills during the years and sodium scales have become a bigger issue. They now cause most of the scaling problems in black liquor evaporators (Schmidl & Frederick 1998). The salts sodium carbonate (Na_2CO_3) and sodium sulphate (Na_2SO_4) are introduced into the pulping process in the digester where cooking chemicals react with wood raw material. The solubility of these salts has an inverse temperature dependency (*Figure 2.4*), thus having the lowest solubility closest to the heat transferring surface where the temperature is the highest (Gourdon 2009). They will therefore precipitate close to the heat transfer surface and are thus likely to adhere to the surface instead of remaining in the bulk.

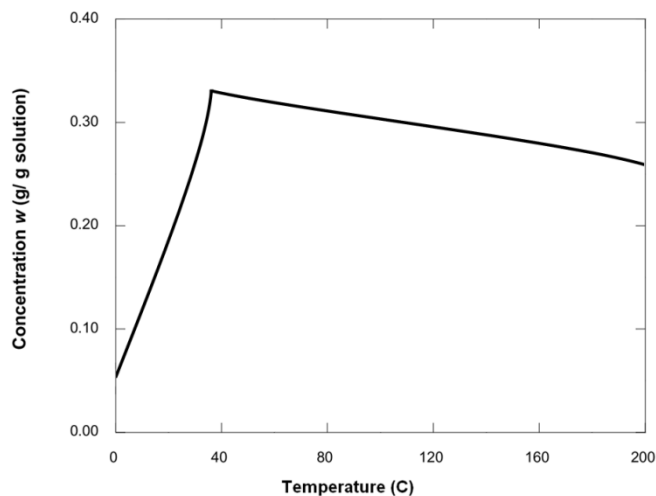


Figure 2.4 A schematic sketch of the solubility of burkeite, sodium sulphate and sodium carbonate. For temperatures above 35 °C the solubility has a more or less inverse temperature dependency (Shi 2002).

Sodium sulphate and sodium carbonate form the double salts burkeite ($2\text{Na}_2\text{SO}_4 \cdot \text{Na}_2\text{CO}_3$) and dicarbonate ($\text{Na}_2\text{SO}_4 \cdot 2\text{Na}_2\text{CO}_3$) when crystallising (Chen & Gao 2004). The exact composition can vary from 1:3.5 to 1:1 moles Na_2CO_3 per mole Na_2SO_4 for burkeite and from 1.5:1 to 3:1 for dicarbonate. Which salt that is formed and its composition depends on the concentrations of Na_2CO_3 and Na_2SO_4 in the solute (*Figure 2.5*).

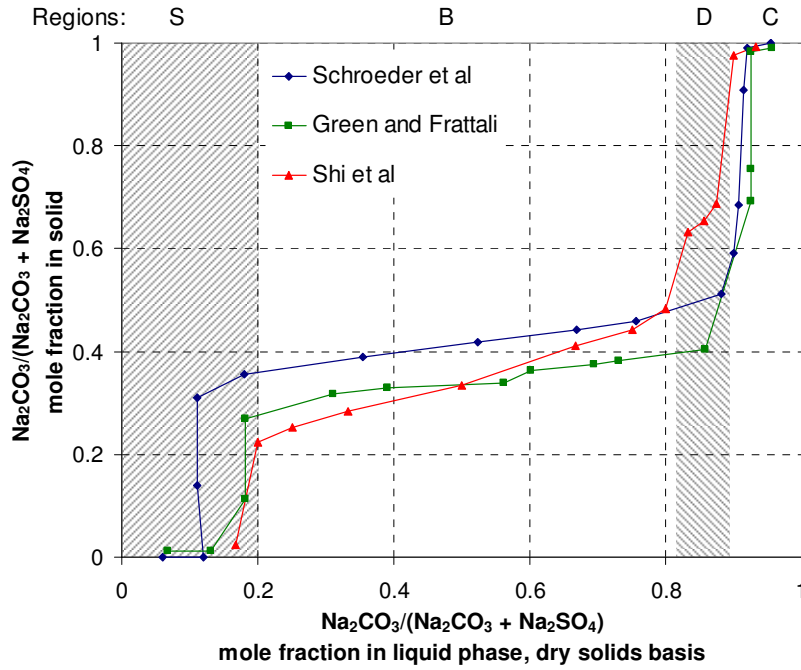


Figure 2.5 Compositions regions for the formed crystals as a function of different solute compositions for aqueous solutions. The four crystal regions are sulphate (S), burkeite (B), dicarbonate (D) and carbonate (C). Equilibrium data from Schroeder et al. (1936), Green et al. (1936) and Shi et al. (2003). Figure adapted from Gourdon (2009).

The relationship x between the two salts sodium carbonate and sodium sulphate is expressed as

$$x = \frac{n_{\text{Na}_2\text{CO}_3}}{n_{\text{Na}_2\text{CO}_3} + n_{\text{Na}_2\text{SO}_4}} \quad (2.5)$$

Equation 2.5 can be rewritten into

$$m_{\text{Na}_2\text{CO}_3} = \frac{x}{1-x} \frac{M_{\text{Na}_2\text{CO}_3}}{M_{\text{Na}_2\text{SO}_4}} \cdot m_{\text{Na}_2\text{SO}_4} \quad (2.6)$$

The proportion between sodium sulphate and sodium carbonate can be altered in order to achieve the desired crystal specie. Generally, the dicarbonate region should be avoided since dicarbonate causes the most severe fouling (Frederick, Verrill, et al. 2004a). During evaporation, more than one type of crystal can form since the solution composition changes as crystallisation occurs. If the process initially is in the burkeite region a shift towards the dicarbonate region will occur as burkeite crystallises and the sodium sulphate concentration decreases in the solution. This comes as a consequence of the crystals having a lower carbonate content than the solution it is crystallising from. If instead dicarbonate is formed, the crystallisation process will shift to the right in Figure 2.5 towards the carbonate region, but when the boundary is reached both carbonate and dicarbonate will crystallise and the solution concentration will be maintained (Shi 2002).

Burkeite crystals are initially very small but agglomerate rapidly to larger crystals. Dicarbonate also starts as very small crystals but as a higher level of supersaturation is reached, more crystals are formed upon primary nucleation. Such crystals have a slower growth rate and agglomerate slower. This together with the large amount of

small crystals makes it more likely for dicarbonate than burkeite to adhere to heat transfer surfaces (Frederick, Verrill, et al. 2004a).

Frederick et al (2004a) have identified two mechanisms for the formation of sodium scales during evaporation of black liquor: primary nucleation followed by agglomeration of the fine crystals on heat transfer surfaces and crystal growth from a supersaturated solution in the metastable region. Both can simultaneously contribute to scaling in the same evaporator effect. As long as the solution is supersaturated scales already attached to the heat transfer surfaces will continue to grow (Frederick, Verrill, et al. 2004a). However, how scales adhere to a clean surface is not completely known. One likely mechanism is agglomeration of the fine crystals formed by nucleation on the heat transfer surfaces. There is some evidence indicating that burkeite crystals can nucleate on a surface, whereas dicarbonate crystals form in the bulk and then adhere to the surface (Euhus 2003).

As mentioned previously in this section, the carbonate to sulphate ratio in the solution changes when sodium carbonate and sodium sulphate crystallise. As a result, different crystal species will form during evaporation. Shi (2002) concluded that if the solution initially was within the dicarbonate region, dicarbonate was the first specie crystallising and forming agglomerates. When the carbonate content in the solution increased during evaporation, sodium carbonate monohydrate started to crystallise. The sodium carbonate crystals had a core of dicarbonate, indicating secondary nucleation with the small dicarbonate crystals working as seeds. Two nucleation points, one for each species, are thus obtained. The first nucleation point will occur when dicarbonate starts to precipitate and the second nucleation point will occur further along the evaporation when carbonate crystallises. The same applies if the solution instead has its starting point within the burkeite region. First, burkeite will precipitate and later on during the evaporation dicarbonate will crystallise, giving two nucleation points (Shi 2002).

2.5 Foulant cleaning procedures in the pulp industry

As previously mentioned in *Chapter 1*, there has been extensive research on the phenomena of fouling and how to minimise it (Müller-Steinhagen 1997; Chen & Gao 2004; Verrill & Frederick 2005; Gourdon 2009) but not so much on how to efficiently remove scales in black liquor evaporators. In 1970 W.R. Grace & Co. patented a method for inhibiting scale formation on metal surfaces of an evaporator and to remove already formed deposits from the mentioned surfaces. By adding a water-soluble polymer to the black liquor during operation scale formation was prevented and existing fouling layers were removed. The main advantage of this method is that scales can be removed without shutting down the evaporator, thus keeping it in operation mode all time (Engman & Clark 1970). Probable drawbacks are the additional cost and labour required when introducing a new chemical into the process and the mill. Furthermore, it is unclear how the additive will affect the recovery process with the recovery of cooking chemicals. Thus, a method easier to implement is a more desirable option.

As mentioned in *Section 2.4.1*, there are two types of scales: soluble and insoluble. Soluble scales, such as burkeite and dicarbonate, are soluble in hot water whereas insoluble scales, e.g. calcium carbonate, require other solvents in order to be removed. Traditionally, insoluble scales have been removed with acid wash or high pressure

water cleaning, the latter also called hydro-blasting (Konopa 1997). Hydro-blasting is often performed to remove the bulk of the deposits before any chemical cleaning methods are applied (Clay 2008). There has also been extensive research on how to prevent calcium scales to form on the heating surface by preheating the black liquor before entering the evaporator (Engman & Clark 1970; Eneberg et al. 2000; MacAdam & Parsons 2004).

Sodium scales are currently removed by periodically boiling out the effects with fresh water, condensate or weak black liquor. The boil-out can be performed without shutting down the whole evaporator by bypassing the effect that is cleaned. The key factor to achieve an efficient boil-out is to reduce the concentrations of the scaling species below the solubility limit and to maintain those low concentrations for a sufficient period of time. No general data have been found regarding how long this period should be. The resulting boil-out liquor will have a high content of dissolved scales, such as Na^+ and CO_3^{2-} , and is gradually re-circulated back into the feed stream. To avoid accumulation of the scale species, the boil-out liquor should be fed slowly back into the feed stream, otherwise there is a risk of enhanced nucleation rate and rapid scaling of the evaporators (Clay 2008). Apart for Clay (2008), no information on how to perform boil-outs has been found. This lack of information makes the efficiency of the boil-outs highly dependent on the skill of the executor. Hence, there is a need for basic knowledge of the dissolutions process of sodium salts in order to create general guidelines regarding efficient evaporator washing.

2.6 Modelling of scale removal in other industries

Cleaning of foulants in other industries than the pulp and paper industry has been investigated by various researchers with the aim to optimise the use of wash liquid and reduce waste. The focus in these studies have mainly been on cleaning tank vessels and the insides of tubes within the food processing industry where cleaning of process equipment is crucial (Grant, Webb, et al. 1996; Grant, Perka, et al. 1996). The results from different cleaning studies have been explained by kinetics, diffusion or chemical reaction models with various degree of success. Depending on which conditions the cleaning process is performed at, either convective mass transfer, diffusion or reaction can be the rate limiting factor (Changani et al. 1997).

The dissolution of a solid into a liquid film is a common process and the rate of solid removal is generally describe as a first order reaction with the difference in concentration between the solid-liquid interface and the bulk of the liquid as the driving force (Kramers & Kreyger 1956):

$$\frac{dM}{dt} = kA(c_i - c_b) = rA \quad (2.7)$$

The total mass of the solid specie M , i.e. the scaling layer, will decrease in time as mass is dissolved and transported from the surface. The driving force for the mass transport is the difference in concentration between the solid-liquid interface, c_i , and the bulk of the solvent, c_b . k is a rate constant and A is the surface area of the solid-liquid interface. Similar expressions where the transport coefficient k is expressed as the diffusion coefficient divided by the boundary layer thickness were developed over 100 years ago (Noyes & Whitney 1897; Nernst & Brunner 1904) and are still used. Common for these expressions is that the dissolution process is assumed to be limited by the diffusion rate of liquid solvent into the solid crystal lattice structure which is

broken up (Dokoumetzidis & Macheras 2006). Equation 2.7 can also be interpreted to describe the transportation of dissolved ions from the crystal lattice out in the solvent by diffusion (Murray 1987; Grant, Webb, et al. 1996; Grant, Perka, et al. 1996).

In an early study by Jennings (1959) the cleaning of milk foulants from stainless steel discs using sodium hydroxide as wash medium was investigated. The relative amount of soil remaining on the discs was reduced following first order kinetics (*Table 2.2*). Furthermore, at a constant sodium hydroxide concentration the rate of soil removal decreased in time, implying that the wash medium is saturated. It was also clear that a higher temperature on the wash liquid reduced the cleaning time significantly (Jennings 1959).

In 1987 Murray proposed a diffusion-reaction model (*Table 2.2*) for the dissolution of metal oxides in relation to the contamination of nuclear reactors. The dissolution reagent diffuses from the bulk flow towards the surface of the oxide layer where it reacts with the metal oxides. The dissolved metal oxides then diffuse back out into the bulk. This results in three rate constants; one for the reaction at the surface and one each for the diffusion of dissolution reagent and of dissolved metal oxide species, respectively (Murray 1987).

Grant, Perka et al (1996) investigated the removal of behenic acid at different temperatures and flow rates using ethanol and a rotating disc apparatus that mimicked the mass-transfer coefficients of a falling liquid film. A diffusion-based mass transfer model was proposed (*Table 2.2*) to describe the process and could in some cases successfully predict the experimental data. The model managed to describe how the cleaning rate depended on flow rate but did not fully reveal the temperature dependency. One suggested reason for this was the assumption of a smooth surface. The real surface was found to be uneven and rough, giving both an increased surface area and enhanced turbulence in the film at the surface. Furthermore, the diffusion was only assumed to occur in one direction: scale into solvent, i.e. no solvent is assumed to be present within the layer. In contradiction, the authors could during the experiments observe a spongy behaviour of the scaling species, indicating that solvent in fact had diffused into the scaling layer. All factors mentioned will result in a higher mass-transfer than predicted by the model (Grant, Perka, et al. 1996). Thus, the porosity of the scaling layer might have a significant effect on the dissolution process.

The removal of calcium phosphate deposits from stainless steel tubes have been studied by Grant, Webb et al (1996) at different pH and flow rates. A mass transfer model based on dissolution behaving as a diffusion process was suggested to describe the removal. However, low accuracy with experimental data resulted in a modified first order model (*Table 2.2*) that considered both dissolution and the mechanical effects that originates from the shear stress (Grant, Webb, et al. 1996). The diffusion model tended to overestimate the rate of removal of deposits, whereas the first order model followed the experimental data well. The first order model was fitted to the experimental data by adapting the constants α and n , and therefore indirectly took into account any mechanism involved in the cleaning process. No clear physical expression for the mechanical effect was presented in their work.

Table 2.2. Literature overview of suggested models describing removal of deposits found in various industries.

Deposit type	Model	Notations	Reference
Dried milk	$\frac{dc_x}{dt} = -kc_x c_{OH}$	Limited by 1st order reaction. Only valid up to 60 % removal of the initial contamination.	(Jennings 1959)
Dirt and scales in condensers	$\frac{dM}{dt} = -k\tau x_{scale}$	Limited by kinetic energy of the fluid and scale thickness.	(Kern & Seaton 1959)
Metal oxides	$\frac{dM}{dt} = -k_1$ $\frac{dM}{dt} = -kM$	Limited by dissolution. Zero order when having a dense film with no pores. 1st order when porous film.	(Murray 1987)
Solid behenic acid residue	$\frac{dM}{dt} = -kA(c_s - c_b)$	Removal occurs by diffusion. 1st order.	(Grant, Perka, et al. 1996)
Calcium phosphate	$\frac{dM}{dt} \propto v_z^b$ $\frac{dM}{dt} = -kM \rightarrow$ $M(t) =$ $M_0 \exp[\alpha v_z^n (t - t_0)]$	Dissolution model. If diffusion sole mechanism: $b=0.86$. First order model, accounts for mechanical removal as well as dissolution. α and n are constants based on experimental data.	(Grant, Webb, et al. 1996)

Of the studies presented above, the work by Grant, Perka et al (1996) is especially interesting since they tried to imitate falling film conditions in their experiments. Furthermore, interesting mechanisms for dissolution of scaling is seen to be diffusion or a combination of diffusion and reaction at the solid-liquid interface. In the work of Jennings (1959) the dissolution rate was modelled as a pure reaction only dependent on the concentration of sodium hydroxide. A more realistic scenario is to include a diffusion term in addition to the reaction term which limits the transportation of either fresh solvent to the scaling surface or the transportation of dissolved ions out in the bulk flow. Equation 2.7 will further on in this study be interpreted as describing the transportation of dissolved ions from the surface of the solid layer into the solvent. This master thesis will be limited to only investigate how the dissolution process is affected by temperature of the wash liquid and wetting degree, even though the previous studies also suggest pH and porosity as possible parameters.

3 Experimental setup and work

To experimentally investigate how the dissolution of sodium scales in a falling film evaporator behaves, a pilot plant at the division of Heat and Power Technology at Chalmers was used. Each experimental run consisted of two parts: a scaling layer build-up and a washing. During the scaling part, a saline solution of sodium sulphate and sodium carbonate dissolved in deionised water was evaporated until a sufficient scaling layer had formed on the heat transfer surface. In the washing part, deionised water at different temperatures and wetting degrees was introduced into the evaporator and the removal of the scaling layer was measured and observed.

3.1 Scaling layer build-up

3.1.1 The pilot plant

The pilot plant was built in cooperation between Chalmers University of Technology and Metso Power AB in 2004. It has been designed to provide results applicable to industrial scale even though its size is significantly smaller than evaporators found at pulp mills. A picture of the plant can be seen in *Figure 3.1*.



Figure 3.1 The evaporator pilot plant from outside the facility.

The evaporator consists of a single tube and is of a falling film type, with the saline solution on the outside of the tube and hot steam on the inside. The tube is mounted vertically and is 60 mm in outer diameter, 4.5 meter long and has a heat transfer surface of 0.848 m². The tube wall thickness is 5 mm. To ensure a uniform falling film a distributor has been specially designed and installed on top of the tube. Since

the evaporator consists of a single tube a system has been developed to return the escaping droplets back to the tube. It is possible to study the falling film through three sight glasses located at 0.6 meter, 2.6 meter and 4.35 meter from the bottom of the tube (*Figure 3.2*).

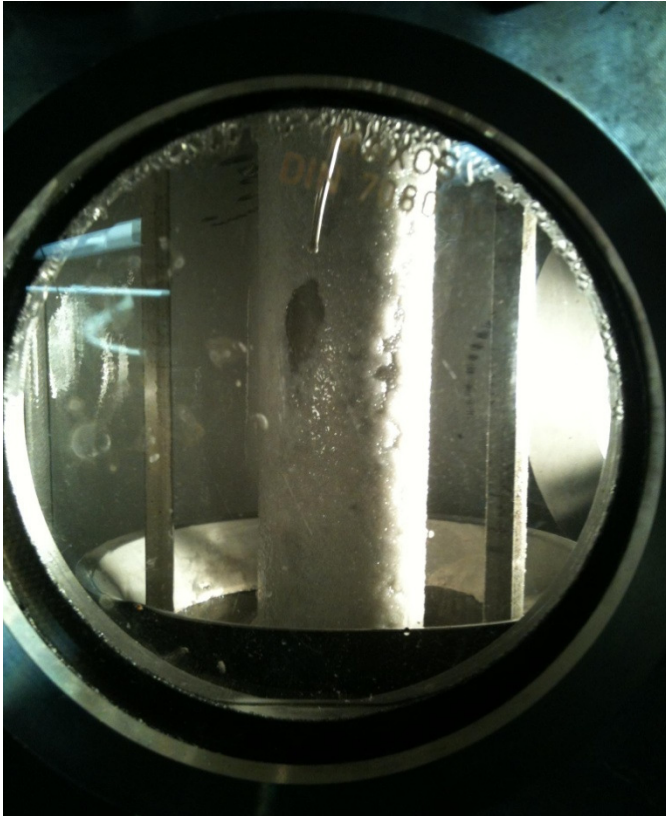


Figure 3.2 The scaling layer covering the tube seen through one of the sight glasses.

Six pairs of thermocouples are mounted along the tube. Each pair is capable of measuring the temperature difference over the tube wall and provides data for the monitoring of the actual temperatures along the tube during operation. The temperature difference is related to the thickness of the scaling layer and can give indications whether the scaling layer is growing or not. The thermocouples paired together are located near the surfaces on the inside and outside of the tube wall. If an insulating scaling layer covers the outside of the tube, the heat flow coming through the tube wall from the steam inside the tube will be hindered and the overall temperature profile will change. But as the insulation layer grows, the temperature difference between the paired thermocouples will level out. A decrease in the temperature difference thus corresponds to an increased thickness. The thermocouples can hence be used as a measurement during the fouling process of whether the scaling layer is growing or not. The thermocouples are, however, not exact enough to provide data for thickness estimations.

In addition to the evaporator, the pilot plant has peripheral equipment necessary for operation. A total process overview can be seen in *Figure 3.3*. The vapour generated during the evaporation is separated from the saline solution in a flash tank and transferred to a condenser. The condensate is pumped into a storage vessel to be used

for after-processing purposes. The concentrated saline solution is re-circulated back into the evaporator. There are two storage vessels with a capacity of 300 litres each available. The saline solution is stored in tank 1 whereas tank 2 is used for collecting the condensate from the condenser.

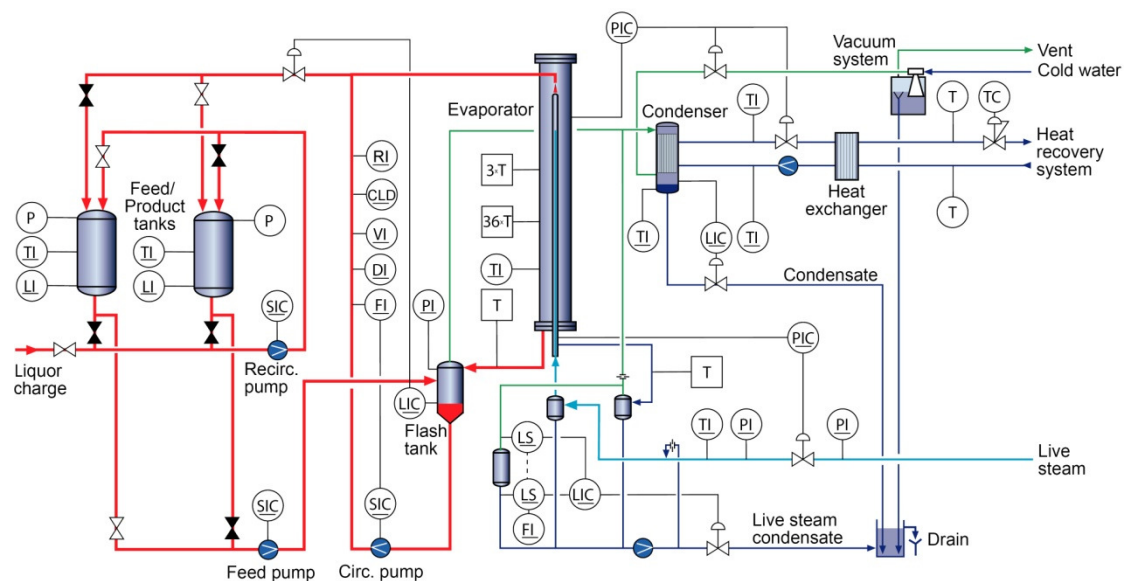


Figure 3.3 Process overview with the evaporator and peripheral equipment.

3.1.2 Operating conditions

In order for both burkeite and dicarbonate to precipitate on the tube wall the mole ratio between sodium carbonate and sodium sulphate in the saline solution must be about 17:3 (*Section 2.4.2*). During precipitation the percentage of sodium carbonate will increase, resulting in a shift in the composition of the formed crystals. Tank 1 was regularly loaded with more salt as an effort to maintain the desired mole ratio, but due to practical limitations it has not been possible to ensure a constant ratio.

The initial concentration level of the saline solution differed between experiments depending on how recently the system had been loaded with salt and if any extracted wash liquid had been fed back into the system. The concentration of the saline solution can be estimated from density measurements using a temperature dependent correlation between density and concentration (*Appendix 1*). A higher initial concentration reduces the time needed for evaporation in order to reach the nucleation point but when the concentration is too close to the solubility limit practical issues with storage will arise. The initial density was around 1120-1230 kg/m³ for all experiments which was well below the solubility limit.

The temperature difference between the steam and the saline solution was slightly higher than normally found in industry. As a consequence, the scaling on the tube wall occurring after passage of the metastable limit was enhanced. The pressure was assumed to have negligible impact on the scale formation and atmospheric pressure inside the evaporator made the washing procedure easier. Hence, the pressure inside the evaporator was chosen to be close to atmospheric pressure when the build-up of the scaling layer was completed. Due to boiling point elevation (*Section 2.1.1*) the pressure was initially slightly higher than atmospheric pressure. The temperatures of the saline solution and steam were therefore decided by the desired pressure and

temperature difference. The steam entering the effect passes through a small steam drum to ensure that it is saturated. Operation parameters for the scaling layer build-up are listed in *Table 3.1*.

Table 3.1. Operation conditions for the scaling layer build-up.

Temperature difference (°C)	Steam pressure (bar, <i>a</i>)	Temperature steam (°C)	Temperature saline solution (°C)	Wetting degree (kg/ms)
15	2	122	107	1.01

When scaling on the tube occurs, crystals will be removed from the solution. Depending on the crystallisation and the evaporation rate, the density of the solution will more or less be maintained and close to the metastable limit. If crystals instead are formed in the bulk of the solution without adhering to the tube, the density will increase and crystallisation in the bulk will be further facilitated. To achieve a rapid scaling and avoid creating crystals in the bulk flow the concentration of the saline solution should be just below that of the nucleation point. To maintain a favourable density the concentrated saline solution is diluted with saline solution from tank 1.

The density of the saline solution was raised during the course of evaporation and at a sufficient density level the first nucleation point (*Section 2.4.2*) was reached with the commencement of precipitation of crystals. The formed scaling layer worked as an insulation material with inferior heat transfer as a result. The thickness of the scaling layer can therefore be related to the overall heat transfer coefficient, below referred to as the k-value, which is calculated based on the amount of condensed steam. During the build-up of scales the k-value will decrease and can be used as an indication of the status of scaling process. If the k-value levels out the density can be further increased up to the second nucleation point to resume the scaling process. The evaporation process continued until the k-value had decreased from its initial value of 2000 W/m²K down to approximately 500 W/m²K. The temperature difference over the tube wall measured by the thermocouples was monitored as well to ensure scaling had occurred over most part of the tube. When the surface around a thermocouple is fouled the temperature decreases due to the inferior heat transfer, thus the temperature difference should first decrease and then level out to ensure that a scaling layer has been formed and no significant scaling occurs any more.

Before the plant was shut down the flow of saline solution over the tube was temporarily stopped to visually observe the scaling layer and determine if it was sufficient for the following washing procedure. During the visual inspection the thickness of the scaling layer was studied together with the distribution of the scales and how much of the tube that was covered with scales. Scales start to form at the bottom of the tube and grow upward towards the top of the tube. Therefore, it is important to check the layer on several positions along the tube. The three sight glasses were used for this procedure.

3.2 Washing

When a sufficient scaling layer had been built-up, the evaporation was stopped and the washing part started. Deionised water of different temperatures was used as wash liquid.

3.2.1 Method

The wash liquid was heated to desired temperature using an electrically driven heating barrel. The heating barrel was placed above the top of the tube and the wetting degree was regulated with a control valve at the bottom of the heating barrel. The wash flow was thus driven by gravity. The initial level in the heating barrel was the same in all experiments. The wetting degree was calibrated on forehand on a clean tube and then measured during the experiment.

To monitor the removal of scales, video cameras were mounted at each sight glass and the entire washing process was recorded. The video films supplied information of how the scales were removed, whether they were evenly dissolved or if there were parts of the tube that became clean sooner, if the flow of wash liquid covered the tube or not, when the tube was clean at the bottom and middle sight glasses and also an alternative way to estimate the thickness of the scaling layer. In addition, the cameras documented any commentary made during the experiment.

To further monitor the removal of scales a device for measuring the scale thickness before, during and after washing was constructed. It was installed next to the bottom and middle sight glasses between experiment 4 and 5. The measurement equipment consists of a small flat disc that is fixed on the end of a metal rod, the disc being perpendicular to the metal rod. The metal rods are mounted in already existing holes in the evaporator shell. When performing a measurement, the metal rod is pushed inwards until it reaches the surface of the scaling layer and is then fixed in position with a screw-nut. Vernier callipers are used to measure how far in the metal rod have been pushed. The obtained value is compared with a reference measurement made when the tube is clean, thus giving the current thickness of the scaling layer. The thickness measurements provide important data concerning the distribution of scales prior to and during the washing. The estimated accuracy of these measurement devices is ± 0.3 mm. The devices are located on different radial position and efforts were made to minimise the contact time with the scaling layer, thus the measurements are considered to have a very small impact on the wetting degree and the cleaning process.

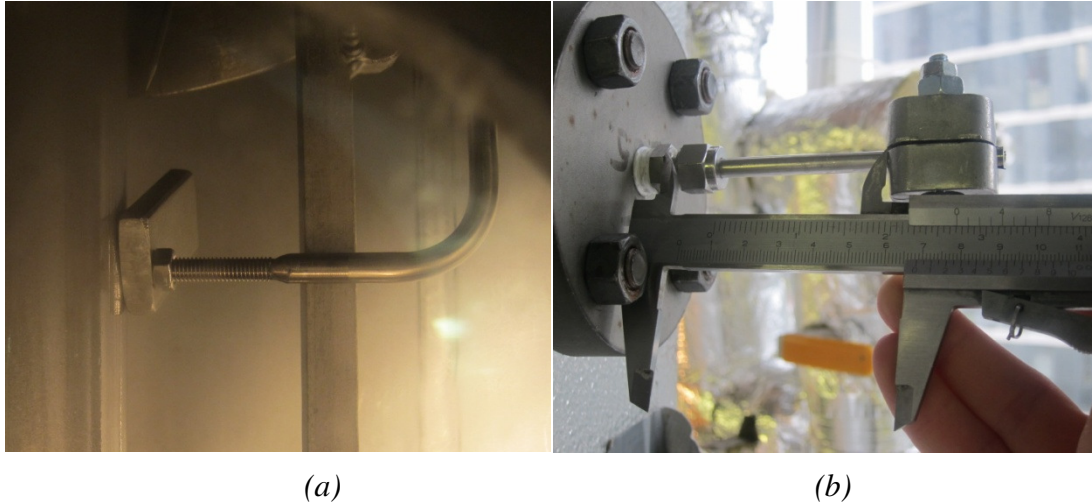


Figure 3.4 One of the two devices constructed to measure the thickness of the scaling layer covering the tube, (a) inside the evaporator and (b) measurement procedure on the outside.

During the scaling part, scales were also formed on other places than the tube, especially at the bottom of the evaporator. Since these scales were not adhered to the tube, they should not be included in the study and hence not be dissolved in the wash liquid. To remove some of these scales and thus improve the accuracy of the results the bottom of the evaporator was flushed with deionised water prior to the washing part. Any plugging of valves or pipes was also dissolved in the process.

To obtain accurate results it is important that the temperature of the wash liquid is kept as constant as possible during the washing process. Depending on the desired washing temperature, the tube needed to be more or less cooled. When the scaling layer build-up phase was stopped the tube had an average temperature of 105 °C. To reach the desired temperature range of 45-85 °C, the tube was cooled from the inside with tap water.

The washing was said to start when the valve to the heating barrel was opened. When the wash liquid had passed the tube it was collected in plastic containers of one litre, each container composing one wash segment. The time it took to fill each container was noted together with the temperature of the exiting wash liquid. The thickness of the scaling layer was simultaneously and repeatedly measured at the two sight glasses as long as scales remain on the tube. When the tube was visually determined to be clean the flow of wash liquid was stopped and the experiment ended. An additional stopping criterion was that the density should not change between wash segments and be close to the density of the ingoing wash liquid.

After the experiment, temperature, density and weight of each wash segment were measured. To verify the concentration estimations made from the density and the temperature, dry solid content was evaluated for a selection of the wash segments in separate analyses where a sample of the wash segment was dried and the remaining salt content was weighed.

3.2.2 Parameters and limitations

To evaluate how the dissolution depends on temperature and wetting degree, different combinations of high and low temperatures as well as wetting degrees were tested. The temperature on the wash liquid was limited to 85 °C due to the capacity of the heating barrel. Since burkeite and dicarbonate have poor solubility below 40 °C, temperatures in the range 45°C to 85 °C were desirable to investigate. This interval is also in the region of the warm and hot water systems at pulp mills and is thus the probable temperature range of the wash liquid that will be used. Due to existing piping dimensions the valve used when collecting the wash liquid can only handle wetting degrees below 0.43 kg/ms. Higher wetting degrees will result in accumulation of wash liquid inside the evaporator which will lead to discontinuous collection of the wash liquid. Wetting degrees below 0.12 kg/ms resulted in insufficient wetting of the tube. Therefore wetting degrees around 0.14 kg/ms, 0.29 kg/ms and 0.43 kg/ms were investigated.

4 Development of a scale dissolution rate model

4.1 Model suggestions

The removal of a scaling layer containing burkeite and dicarbonate from the outer surface of a tube is considered to be limited by the dissolution of solid into the falling film. Two model suggestions have been experimentally evaluated for the dissolution process. In the 1st order model, the hypothesis is that the dissolution process only depends on diffusion and is therefore modelled with a first order expression (Equation 2.7). In the second model suggestion, the diffusion-reaction model, a reaction term was added to account for the transformation of crystals into ions. Both models assume a bulk flow that is perfectly mixed.

4.1.1 1st order model

In the 1st order model the rate determining dissolution mechanism is considered to be the diffusion of ions from the surface of the scaling layer through a boundary layer and into the bulk flow (Figure 4.1). When the dissolved scales have diffused through the boundary layer they are regarded as part of the bulk flow, thus resistance of mass transport in x-direction can be neglected in the bulk and the bulk concentration will be constant. The concentration at the solid-liquid interface is assumed to be constant and equal to the saturation concentration at the current temperature.

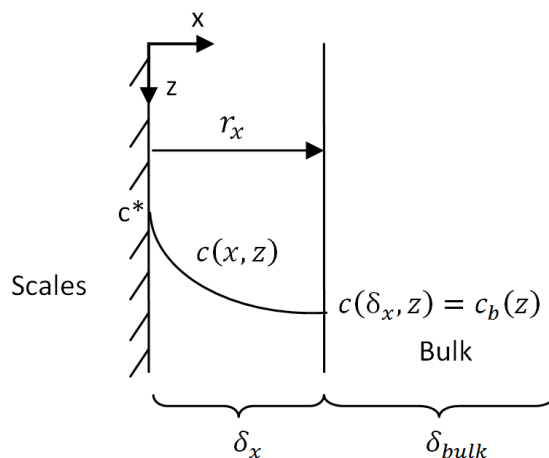


Figure 4.1 Schematic representation of concentration profile in the boundary layer between the solid scales and the wash liquid.

The dissolution of the crystals into free ions in the wash liquid will be dependent on the diffusion rate and if there are any scales left on the tube to be dissolved. The latter will be modelled with a delta function θ that is equal to 1 if scales cover the tube or 0 if the tube is clean. The dissolution rate is modelled as depicted in equation 4.1.

$$r_x = k(c^* - c_b)\theta \quad (4.1)$$

k is a transport coefficient that takes into account the transportation of dissolved scales through the boundary layer between the scaling layer and the bulk flow and thus include the thickness δ_x .

4.1.2 Diffusion-reaction model

A second mechanism in form of a reaction expression can be added to describe the dissolution process and, in particular, the breakage of the crystal structure into ions. The film is therefore divided into a reaction boundary layer in addition to the previous diffusion boundary layer and bulk flow (*Figure 4.2*). The two boundary layers have separate concentration profiles and different thicknesses.

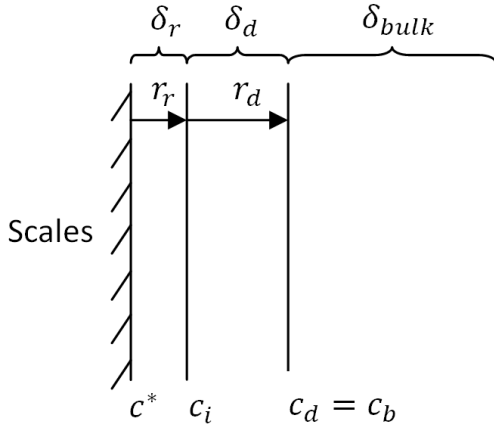


Figure 4.2 Division of the falling film into two separate reaction and diffusion layers and a bulk flow.

In the reaction boundary layer the rate limiting mechanism for the transportation of salt is the transformation of crystals into ions and the process is describe with a reaction expression (*Equation 4.2*). The liberated ions are then transported through the diffusion boundary layer where the transport mechanism is diffusion and modelled according to equation 4.3.

$$r_r = k_r(c^* - c_i)^{n\theta} \quad (4.2)$$

$$r_d = k_d(c_i - c_d) = k_d(c_i - c_b) \quad (4.3)$$

k_r is a reaction coefficient and k_d is a transport coefficient, both will account for the film thicknesses δ_r and δ_d , respectively. The bulk is as before considered to be perfectly mixed, thus the concentration is constant throughout the entire bulk. The reaction-diffusion model represents a coupled system and has to be discretised into small time steps if to be solved.

4.2 Calculation methods

MATLAB was used to model the washing behaviour and dissolution rate. The tube was discretized into several cells in z-direction with rotational symmetry (*Figure 4.3*). The washing was simulated by taking small time steps. All physical properties were assumed to be constant within each cell. Each cell had its own scale thickness which decreased depending on the dissolution rate r .

To simplify the calculations the interfacial area A between the scales and the wash liquid is assumed to be constant and equal to the heat transfer area of the tube. In

reality it will vary depending on the thickness and roughness of the scaling layer. However, the contribution is only at most 5 %, making it a reasonable assumption.

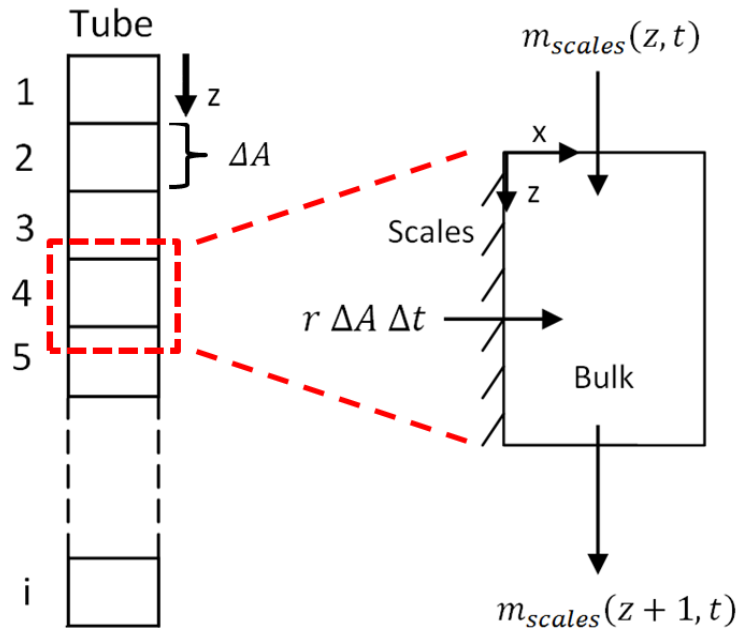


Figure 4.3 The tube was discretized in z-direction into several cells.

The program uses both internal and external mass balances. There are mass balances within each cell to ensure that the amount of salt dissolved from the tube is equal to the amount transported out by the wash liquid. The external mass balance ensures that the assumed distribution of scales adds up to the amount of dissolved scales in all the wash segments.

The mass, concentration and scale thickness for each cell and time step was calculated. The concentration out from the last cell was plotted together with the wash segments' concentrations to study their consistency. The change in scale thickness in the cells corresponding to the middle and the bottom sight glass were plotted together with the scale thickness measurements during the washing. It was thereby possible to study how well the model could predict the dissolution rate. These figures are the main tools when evaluating the performance of the different models and will be further discussed in *Chapter 5*.

4.3 Scale distribution

It is necessary to know the scale distribution on the tube if the washing is to be modelled since it will affect the interfacial area A . Even though the scale thickness was measured at both the middle and the bottom sight glass, the thickness at the rest of the tube was unknown. With a known amount of scales dissolved in each container and approximations of the thickness at the three sight glasses a realistic scale distribution was estimated.

According to previous research (Gourdon 2009), scales grow from the bottom and up. Since the scales acts as insulation material on the tube it is realistic to assume that the

growth will slow down as the layer gets thicker and the heat transfer is hindered. This behaviour was also confirmed during the experiments where the thicknesses of the scaling layer at the two lower sight glasses were about the same. The scales below the bottom sight glass were therefore generally assumed to have the same thickness as the scales in the bottom sight glass. The thickness between the bottom and the middle sight glass was estimated with linear interpolation.

The thickness of the scaling layer at the top sight glass was visually estimated due to the low amount of scales making measurements impractical. The thickness between the middle and the top sight glass was more difficult to estimate due to the relatively long distance of 2 meter and the fact that the thickness varied from about four millimetres down to zero. The scale thickness in this part was approximated with linear interpolation and adjusted to match the amount of dissolved salt in the wash liquid. A typical result of this procedure can be seen in *Figure 4.4*.

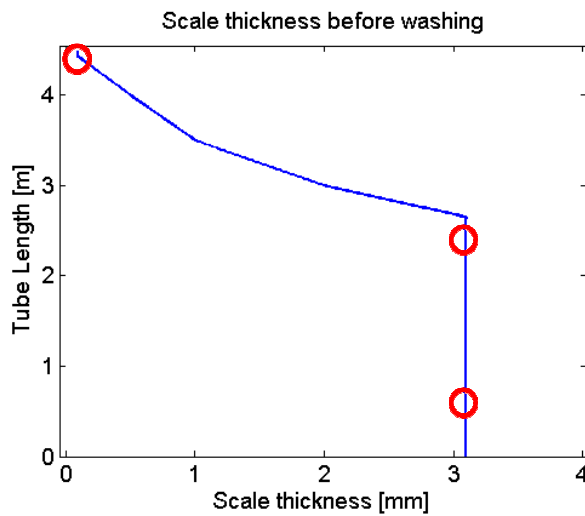


Figure 4.4 A typical estimation of the scale distribution. The thickness at both 0.6 meter and 2.6 meter was measured to 3.1 mm and the thickness in the top was visually determined to be 0.1 mm.

5 Experimental results and discussion

Eight experiments were conducted and are included in this study. In *Table 5.1* experimental conditions are listed together with washing conditions such as amount of salt dissolved in the wash liquid and how much wash liquid that was required to clean the tube. *Table 5.1* also specifies the behaviour, either exponential or inverse S-shaped decrease, of how the salt content varied between the wash segments. More results from all experiments can be found in *Appendix 2*.

Table 5.1 Overview of the performed experiments showing parameter values and general results.

Exp nr	$T_{avg,in}$ (°C)	$T_{avg,out}$ (°C)	Γ (kg/ms)	Salt on the tube (kg)	Water required (l)	Shape
1	40	52	0.157	4.0	24	Exp
2	76	76	0.139	1.8	10	Exp
3	45	48	0.168	2.9	17	S
4	84	81	0.123	3.9	16	S
5	82	78	0.295	3.8	19	S
6	63	75	0.287	3.8	21	S/Exp
7	84	82	0.401	4.4	22	S/Exp
8	63	72	0.432	4.1	24	S

5.1 Washing behaviour

Figure 5.1 shows how the concentration of dissolved scales typically varied between the containers. Each column represents a container of one litre in which a wash segment was collected. The x-axis shows the washing time in minutes and the width of each column represents how long time it took to fill the container with approximately one litre of wash liquid. The columns are usually wider at the end since the volumetric flow varied over time. The variation originated from the volume expansion caused by the dissolved scales (*Appendix 1*). The y-axis shows the amount of dissolved scales per amount of solution. The dashed line represents the solubility limit which indicates the maximum possible amount of salt that can be dissolved in the wash liquid.

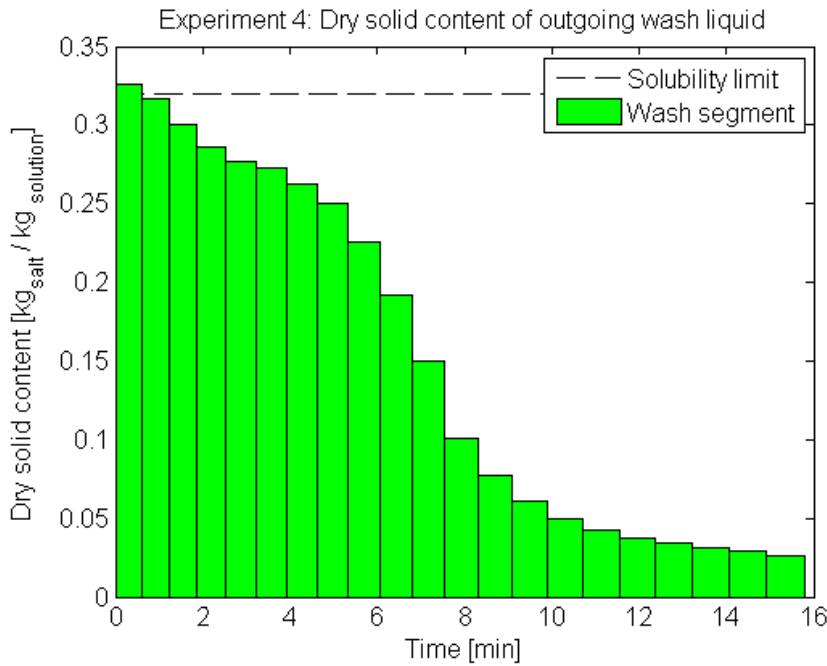


Figure 5.1 Typical washing behaviour where the salt content in the wash liquid decreases with time. Each column represents the salt content of the wash liquid in a specific container.

The concentration of salt between wash segments varied over time, usually formed like an inverse S (Figure 5.1). The content of dissolved salt in the segments varied from a value close to the solubility limit down to a level of only 5 % of the maximum. At the end of the washing the concentration of salt levelled out above zero, i.e. even though the tube was clean the wash liquid still contained dissolved scales. Most likely, a large amount of scales were formed in the bottom of the evaporator and due to insufficient flushing of the bottom (Section 3.2.1), crystals were still present when the washing started. Flushing of the bottom with the same flow rate as during the washing has validated this theory.

The high concentration in the beginning of the washing does not have to be scales dissolved from the tube but could be residual saline solution from other areas. For instance, even though the distributor on the top was drained from saturated solution it is likely that it still contained some residual solution when the washing began. In addition, the flow will not be fully developed in the beginning since it takes time to establish a fully developed flow, especially for high flow rates. During that time, the flow of water was lower than in the rest of the washing allowing it to reach a higher level of saturation. Moreover, as the tube was cooled from the inside to achieve the desired temperature, vapour started to condense on the scaling layer. The tube was therefore usually covered with a thin, saturated layer of water prior to washing.

5.2 Dissolution of scales

The scale thickness measurements during the washing revealed that for all experiments the scales in the middle sight glass started to dissolve rapidly already at the beginning of the washing. The rapid thickness reduction was more or less

persistent throughout the whole washing. The scales at the bottom sight glass started to dissolve with a much slower rate but later increased to the same rate as the one at the middle sight glass.

The washing behaviour can be related to how the concentration of salts varied between the wash segments. Approximately when the tube became clean from scales in the middle sight glass, the outgoing salt concentration started to rapidly decrease and then level out a short time after the bottom sight glass became clean. The outgoing salt concentration changed only as more parts of the tube became clean and not while the scaling layer got thinner. This indicates that the thickness of the scaling layer probably is irrelevant for the dissolution rate and that it is only the surface of the scaling layer that is involved in the dissolution process. When parts of the tube become clean, the contact time between wash liquid and scales will be lower, resulting in less concentrated wash liquid (*Figure 5.2*).

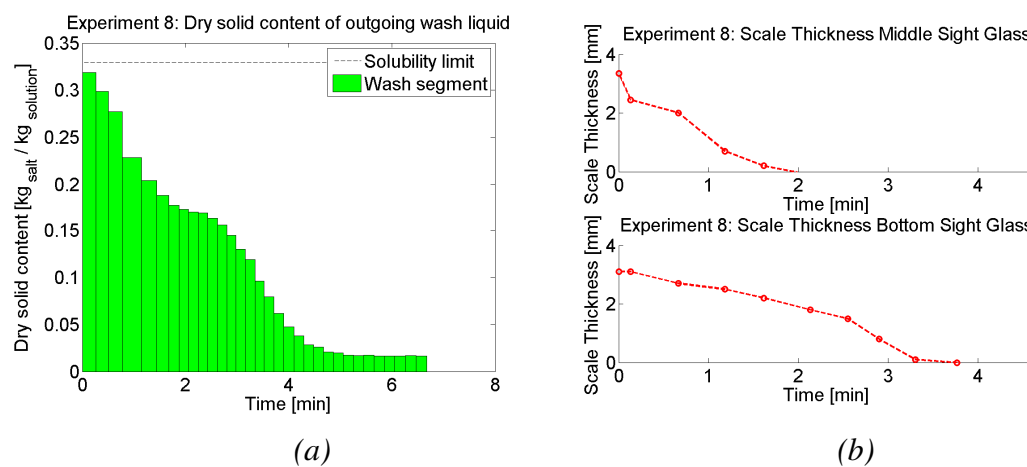


Figure 5.2 (a) A typical appearance of how the salt content in the wash liquid changed with time and (b) thickness of the scaling layer in the middle and bottom sight glass as a function of time where dots represent measurements.

5.3 Temperature and wettability dependence

The washing behaviour differed depending on the physical conditions during the washing, i.e. with the wetting degree and temperature at which the washing was carried out. For a wetting degree around 0.123 kg/ms the wash liquid in all the wash segments contained over 0.25 kg salt per kg solution (80 % of the saturation limit) until the middle sight glass became clean. When the wetting degree was increased to 0.295 kg/ms fewer of the first wash segments had a high saturation degree. The high saturation level in the first segments was probably a combination of the dissolved thin scaling layer at the top of the tube mixed together with residual saline solution as previously discussed. The subsequent wash segments typically levelled out at a concentration of 0.2 kg salt per kg solution until the middle sight glass became clean, at which point the concentration started to decline again. When the wetting degree was doubled from 0.123 kg/ms to 0.295 kg/ms the washing time was cut in half but 19 % more wash liquid was required (*Figure 5.3*).

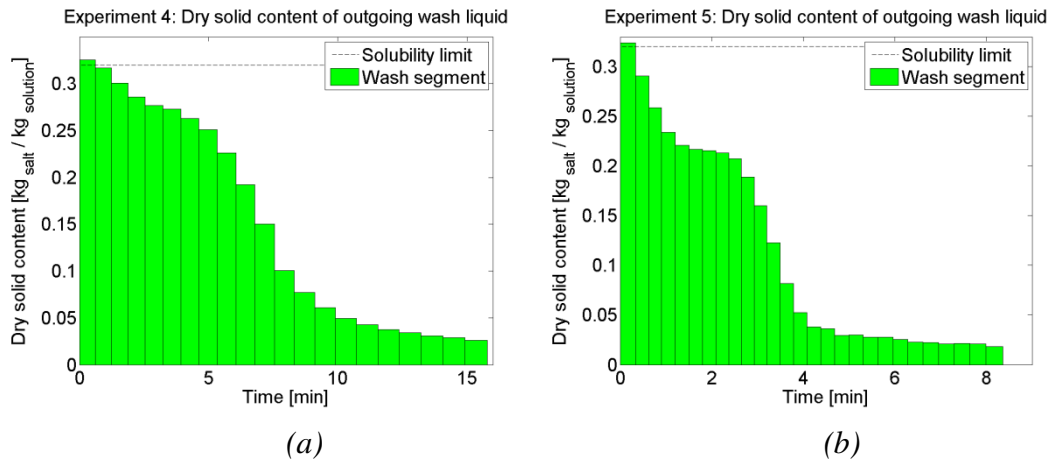


Figure 5.3 The amount of salt dissolved in each wash segment changed when the wetting degree was increased from (a) 0.123 kg/ms in experiment 4 to (b) 0.295 kg/ms in experiment 5.

As mentioned in Section 5.1, the cooling of the tube resulted in vapour condensing on the scaling layer and therefore the cooling was stopped to avoid pre-wetting of the scaling layer. Due to insufficient cooling in experiment 6 and 8, the attempts to reach a lower washing temperature were unsuccessful. Only in experiment 3 a constant temperature below 75 °C was successfully achieved. However, because of the relatively low amount of scales formed on the tube in experiment 3, subsequent experiments were unable to replicate the same conditions at a higher temperature. Therefore it is difficult to conclude how the temperature affects the washing by only comparing different cases.

5.4 Deviating washing behaviour

The washing behaviour for experiment 1 and 2 deviated from the others. The change in concentration between each wash segment followed an exponential curve rather than the previously mentioned inverse S-shape. In experiment 1 the wetting of the tube was uneven which led to an inhomogeneous tube cleaning (further addressed in Section 5.5) and probably caused the different appearance of salt concentration in the wash segments (Figure 5.4). Due to malfunctioning equipment in experiment 2 the evaporation had to be stopped prematurely which resulted in a significantly thinner scaling layer. The low amount of scales on the tube probably caused a different scale distribution which resulted in the exponential washing shape.

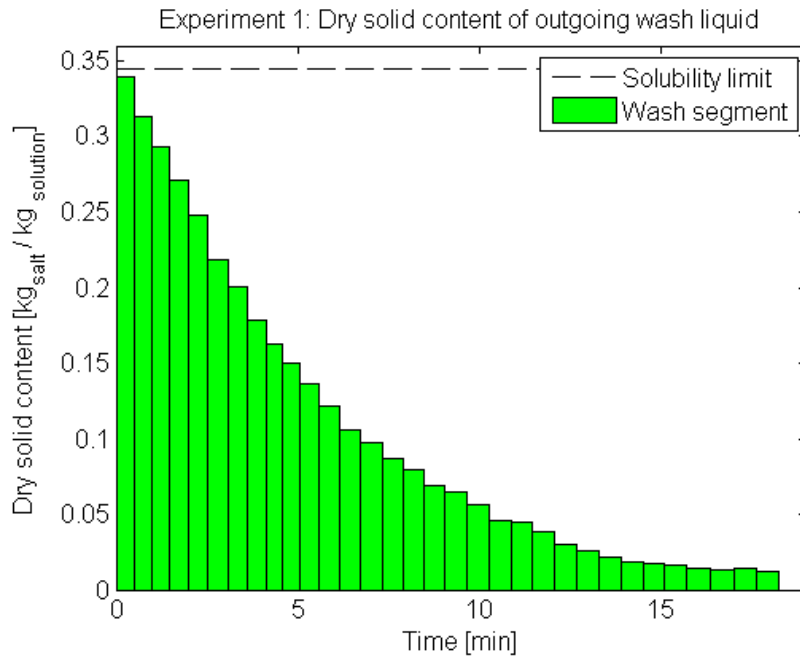


Figure 5.4 One of the deviating experiments showing an exponential decrease in salt concentration.

Experiment 6 and 7 had a washing shape that was a mixture between inverse S and exponential shape. As before, the deviating appearance of the washing curve is believed to be caused by a slightly different scale distribution and a different amount of residual saline solution in the evaporator when the washing began.

5.5 Relevance of wetting degree

During the first experiment the tube was slightly out of vertical centred position making the flow a bit higher on one side of the tube. The resulting uneven washing can be seen in Figure 5.5 where only half of the tube is clean. The right side required twice as much time to become clean compared to the left side. This indicates how important it is to have an even wetting degree around the circumference of the tube.

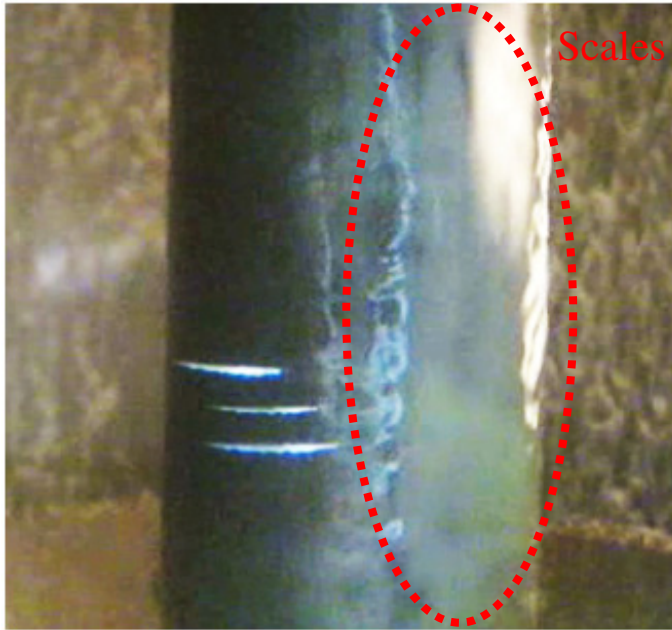


Figure 5.5 Due to an uneven flow in experiment 1, the left side of the tube was cleaned from scale before the right side.

5.6 Scale cracking

Parts of the scaling layer did not dissolve in the wash liquid but were instead removed due to scale cracking. In nearly all experiments fragments of the scaling layer were detached from the tube at the bottom sight glass. The scaling layer started to crack at the end of the washing, either when it became thin enough or when a small part of the tube became clean. The cracking occurred in two different ways: the scales could either become completely detached from the tube and fall off, or it could break loose and slide down along the tube. If they slid along the tube the detached scales facilitated the removal of more scales from the tube by mechanically scraping off the scales further down. Since the scale cracking only occurred at the lower part of the tube and only at the end of the washing it had a marginal impact on the scale removal and was therefore not included in the model.

6 Modelling results and discussion

The variation in dry solids content of the outgoing wash liquid was modelled and compared to the experimental results. A constant transport coefficient for each model and experiment was fitted to the experimental data. It was adjusted so it could simulate the outgoing wash liquid, i.e. match the salt concentration in the wash segments. A perfect match was not necessary for the wash segments in the beginning and at the end of the washing, since it had been concluded that these segments also contained scales from other places than the tube (*Section 5.1*). Therefore, the transport coefficients were adjusted to specifically match the salt content during the middle part of the washing.

6.1 Evaluation

All proposed models simulated the washing in almost the same way for all experiments and therefore only two experiments will be discussed here. How the models simulated the wash segments for experiment 5 can be seen in *Figure 6.1*.

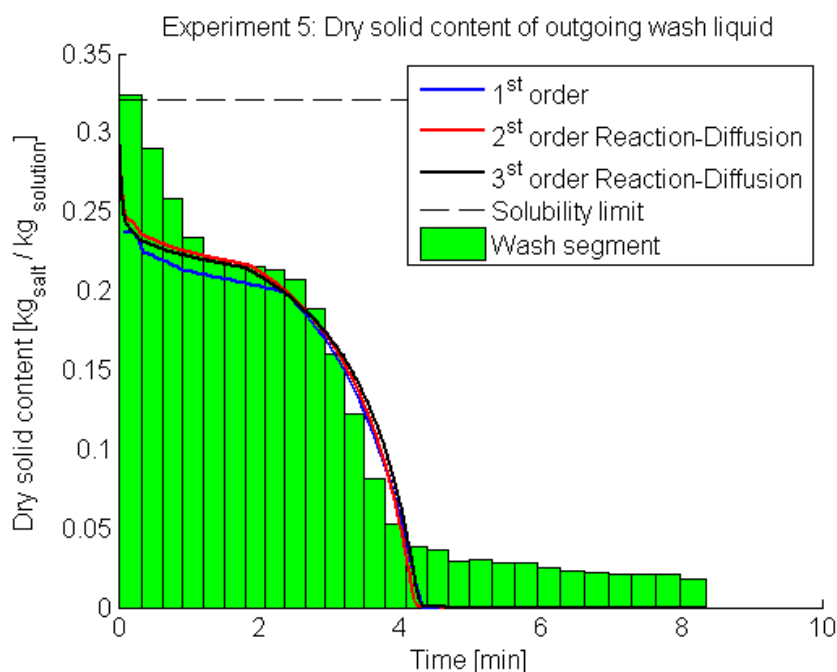


Figure 6.1 Experiment 5 is a typical case on how the proposed models predicted the salt content in the wash segments.

All proposed models were capable of simulating the characteristic washing behaviour with about the same accuracy. The models differed on the other hand from each other when it came to predicting the dissolution rate in each sight glass. As can be seen in *Figure 6.2* the 1st order model provided the best prediction in the middle sight glass. However, it is not obvious for the bottom sight glass. For experiment 5 the 1st order model was the closest to predict when the tube would become clean, but the 3rd order model provided a better match during the washing and only deviated at the end. However, the most important aspect of the model is that it should be able to predict

when the entire tube becomes clean and therefore the 1st order model is regarded as the most accurate model.

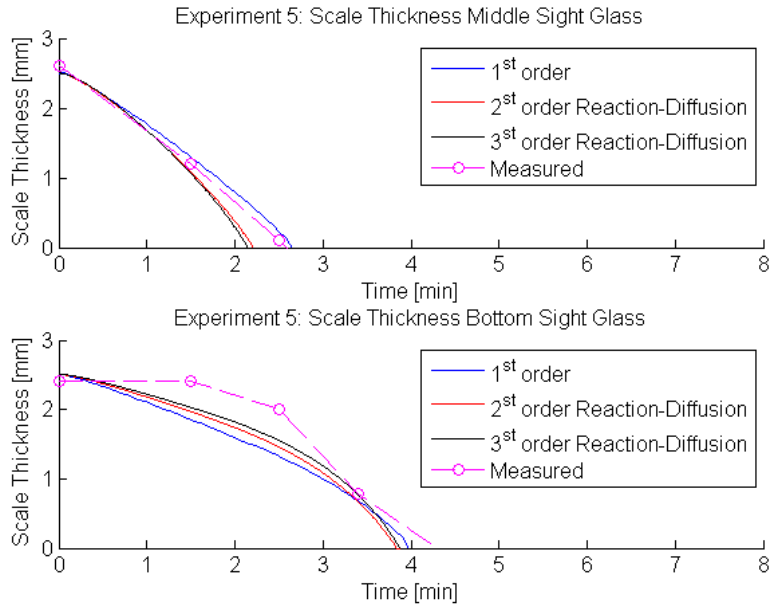


Figure 6.2 The proposed models predicted the dissolution rate differently. How it was predicted was unique for each experiment but the 1st order model was always the most accurate one.

In *Section 5.4* it was discussed that experiments 1 and 2 had a deviating washing behaviour from the others. None of the proposed models were able to predict their characteristics (*Figure 6.3*). Since the scaling thickness was not measured during the washing in these experiments, the models could only be compared to the time at which the tube was visually considered clean (*Figure 6.4*). Due to the lack of data and the deviating behavior it is difficult to tell if the adapted models can be used to simulate the washing in these two cases. If the scale distribution is estimated in another way than the procedure described in *Section 4.3* it is possible to achieve a better fit, but since the real distribution is unknown it is difficult to tell if this approach is more accurate. These experiments have therefore been disregarded from further analysis.

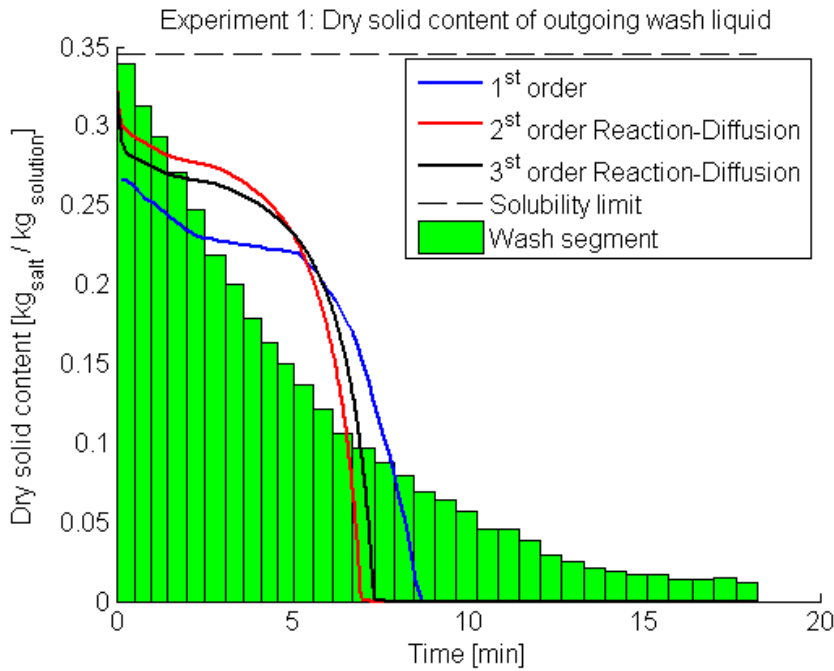


Figure 6.3 None of the proposed models were able to simulate the washing behaviour in experiment 1.

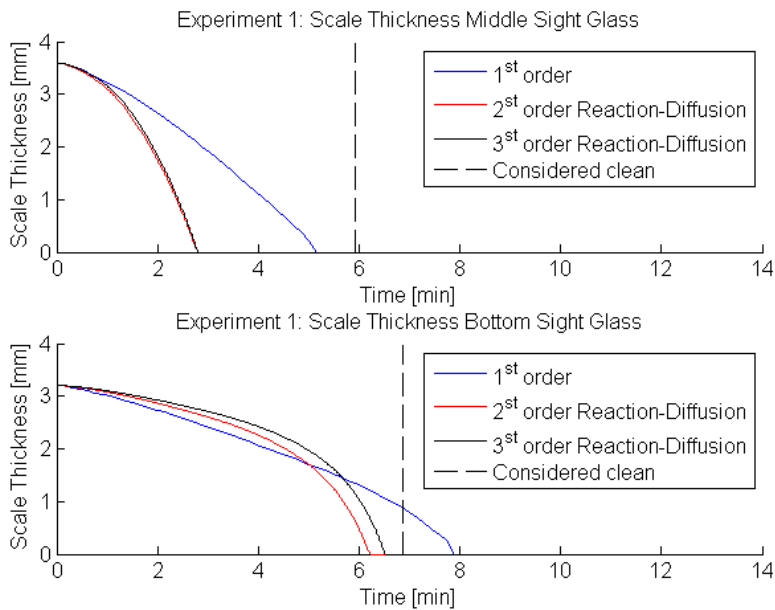


Figure 6.4 Comparison of when the tube is considered clean by the models and from studying the video films in experiment 1.

6.2 Parameter optimisation

Since the 1st order model generally provided most consistency with the measurements in all the experiments further investigation of its transport coefficient was conducted. Table 6.1 shows the value of all the fitted transport coefficient for the 1st order model together with some characteristic experimental conditions.

Table 6.1 Transport coefficients for the 1st order model and some experimental conditions for the modelled experiments.

Exp nr	$T_{avg,in}$ (°C)	$T_{avg,out}$ (°C)	Γ (kg/ms)	k ($\frac{kg_{solution}}{m^2*s}$)
1	40	52	0.157	-
2	76	76	0.139	-
3	45	48	0.168	0.070
4	84	81	0.123	0.155
5	82	78	0.295	0.150
6	63	75	0.287	0.120
7	84	84	0.401	0.160
8	63	72	0.432	0.130

Experiment 4, 5 and 7 had approximately the same temperature but different wetting degrees. By comparing the wetting degrees and the adjusted transport coefficient, no correlation between them is seen (Figure 6.5). This indicates that the transport coefficient is independent of the wetting degree inside the investigated region.

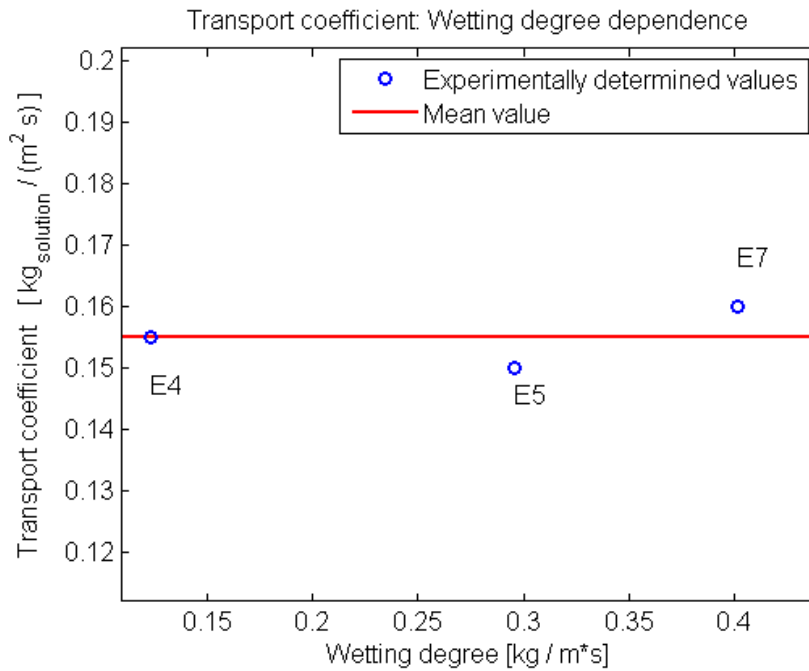


Figure 6.5 No clear dependence between the transport coefficient and the wetting degree is shown.

Experiment 3, 4, 5 and 7 were conducted at stable temperatures (inlet temperature approximately the same as the outlet temperature). If the transport coefficient in these experiments is plotted against the temperature it appears as k varies linearly with temperature (Figure 6.6).

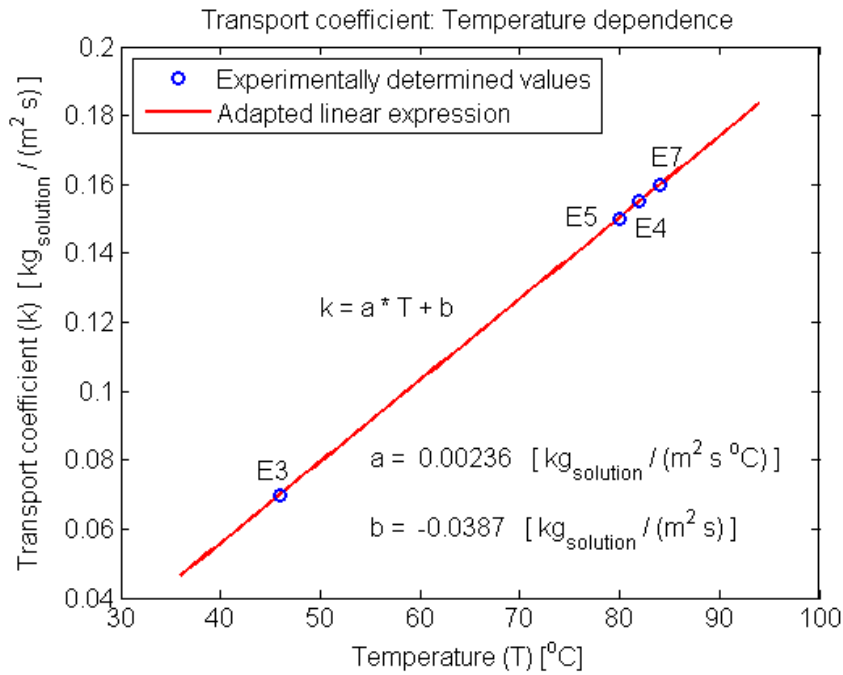


Figure 6.6 A linear expression can describe the temperature dependence for the transport coefficient.

The unit of k is a result of the driving force of the transport mechanism being expressed as mass salt per mass solution. However, k can easily be expressed with the more commonly used unit meter per second if divided by the density of the solution.

The cooling of the tube was insufficient in experiment 6 and 8, leading to large temperature differences between the ingoing and the outgoing wash liquid. The wash liquid also experienced large temperature variations during the wash. To account for these temperature fluctuations and thus improve the model, the constant transport coefficient was replaced by the linear, temperature dependent expression for k . The temperature profile was unknown and therefore it was assumed that the ingoing wash liquid was heated directly to the outgoing temperature. This assumption is reasonable since the tube was the hottest on the top and the absence of scales in this part resulted in a high heat transfer. The modelling of the washing with this method lead to higher consistency with the measurements for both experiment 6 and 8 and the improvements for the latter can be seen in Figure 6.7. This can be regarded as a confirmation of the transport coefficient being temperature dependent.

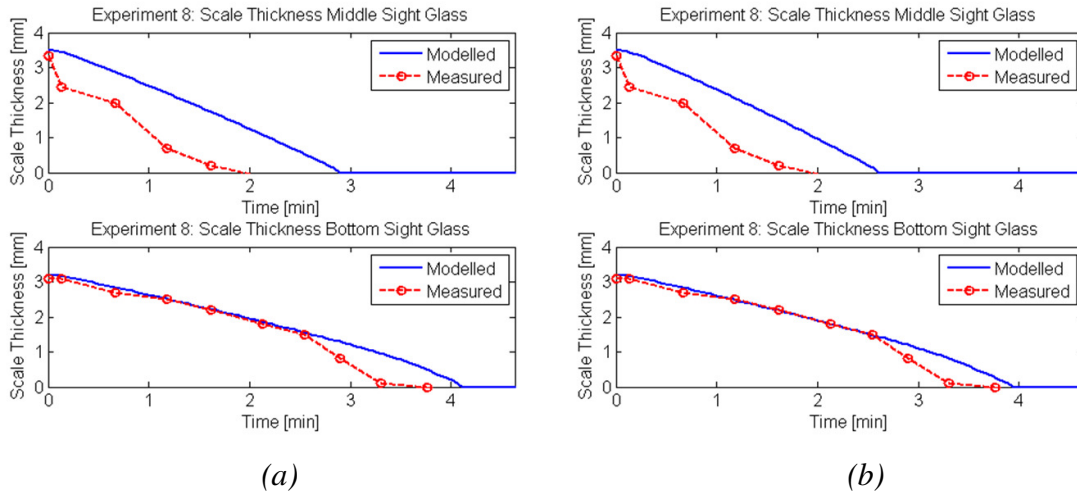


Figure 6.7 The model prediction of the dissolution rate in the sight glasses for experiment 8 with (a) a constant value for k and (b) a linear temperature dependent expression for k .

6.3 Validity of the proposed dissolution model

In other industries than pulp and paper, 1st order models have been proposed to describe cleaning of foulants, and therefore strengthens the choice of this model. 1st order models appear frequently in literature and are used to describe all kinds of physical phenomena.

The limiting transport mechanisms for the dissolution expressed as the 1st order model could be reaction or diffusion. The wetting degrees at which the experiments were conducted yielded Reynolds numbers in the boundary between turbulent and wavy laminar flow up to the more turbulent regions (Table 6.2). Since the flow is mostly inside the transition region between wavy laminar and turbulent, it is difficult to say whether it is reaction or diffusion that is the limiting transport mechanism. Higher wetting degrees need to be investigated in order to determine the limiting mechanism. If the dissolution rate does not increase when the flow is fully turbulent it would indicate that reaction is the limiting transport mechanism. If instead diffusion limits the transport there would be an increase in mass transport with increasing turbulence.

Table 6.2 Reynolds number and thickness of the falling film for the three wetting degrees investigated in the experiments.

Γ	Reynolds number	Estimated
0.145	424	$2.53 \cdot 10^{-4}$
0.290	581	$3.86 \cdot 10^{-4}$
0.435	1361	$4.51 \cdot 10^{-4}$

Even though the exact transport mechanism cannot be determined it can be investigated if the proposed model is realistic by estimating the thickness of the boundary layer using diffusion theory (Welty et al. 2008). Liquid-liquid

diffusivities are typically of the magnitude 10^{-9} m²/s. The modelled transport coefficient is 0.1 kg_{solution}/m²s at 60 °C and the density of the solution is generally 1200 kg/m³. This results in a boundary layer thickness of:

$$\delta_x = \frac{D_{AB} * \rho}{k} = \frac{10^{-9} * 1200}{0.1} = 1.2 * 10^{-5} m \quad (6.1)$$

The magnitude of δ_x is realistic since it is much smaller than the total film thickness which was around 3.5×10^{-4} m (*Table 6.2*).

The proposed temperature dependency, together with the independency of the wetting degree for the transport coefficient, is consistent with existing transport theory (Bird et al. 1960). It should be mentioned that since a lot of physical properties are temperature dependent the proposed temperature relation can be replaced by a function depending on other physical properties. Since the influence of viscosity or any other physical properties has not been investigated it is not possible to distinguish them from each other, thus it is more reasonable to only discuss temperature dependence.

7 Model implementation

The determined dissolution rate model can be used to further understand the washing process. If the model is assumed to be valid even outside the determined region it can be used to investigate how different parameters will influence the washing at sizes relevant for the industry.

When washing with pure water, mainly three parameters influence the washing: wetting degree, temperature and length of the scaling layer covering the tube. The latter may be difficult to estimate but unfortunately it is essential to know since it will have a significant impact on the surface area of the solid-liquid interface. In industry the wash liquid is usually re-circulated over the tube hence it is relevant to also include a fourth parameter namely the salt concentration in the ingoing wash liquid since it might not have to be pure water.

When evaluating how these parameters influence the washing it is practical to use saturation degree. A saturation degree of 0 % means that no salt has been dissolved in the wash liquid whereas a saturation degree of 100 % means that the wash liquid is saturated and no more scales can be dissolved in it. *Figure 7.1* shows how each of the four parameters affects the outgoing saturation degree when the others are kept constant.

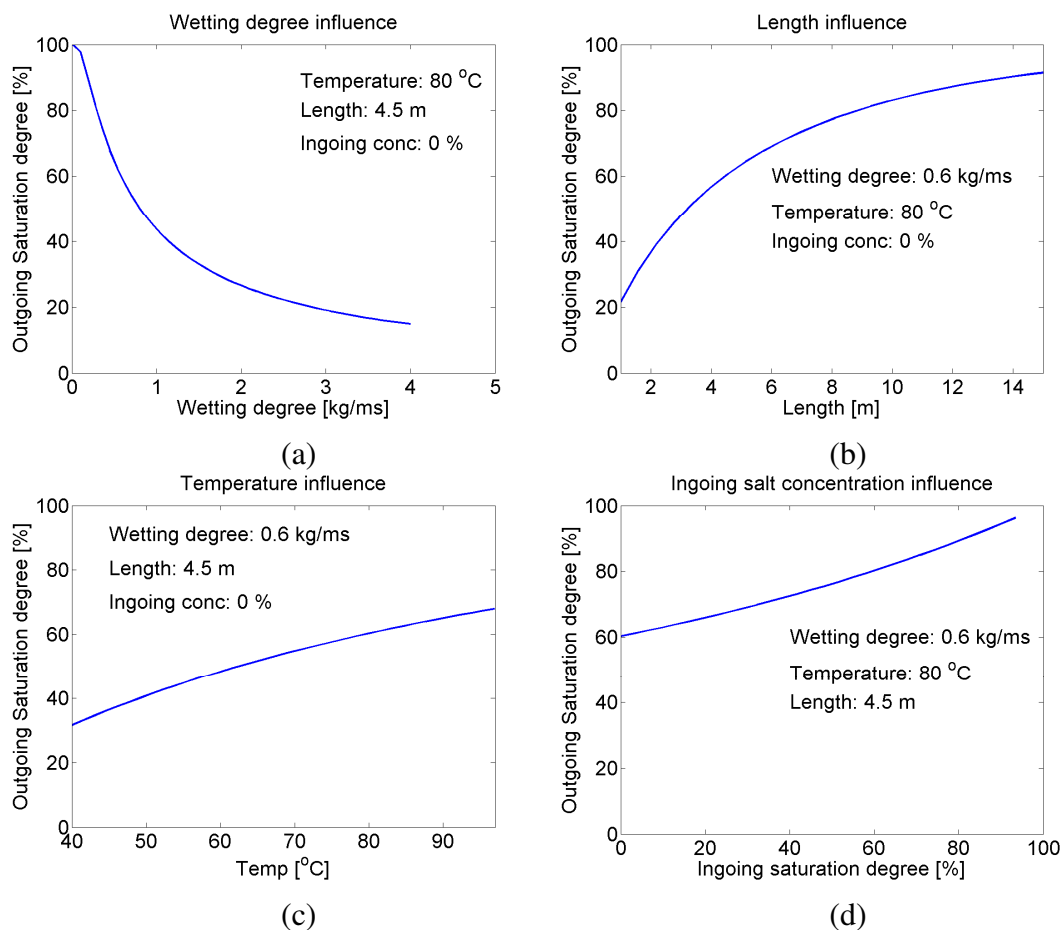


Figure 7.1 How the washing is influenced by: (a) wetting degree, (b) temperature, (c) length of the scaling layer and (d) concentration of the ingoing wash liquid.

By studying *Figure 7.1* it is possible to conclude that all four parameters have quite a strong influence on the washing but some has a larger impact than others. The parameter with the largest impact is the wetting degree. At very low wetting degrees it is possible to achieve a nearly saturated solution but if the wetting degree instead is increased above 3 kg/ms the saturation degree will only reach 20 %. Since the parameters affects the performance of each other the graphs in *Figure 7.1* should only be considered as typical examples.

To fully describe how these parameters influence the washing, three correlations have been developed. It was problematic to construct a single correlation that was both simple and accurate enough to describe the influence of all four parameters. Therefore the ingoing saturation degree was removed and instead three correlations were constructed each at different ingoing saturation degrees. The correlations were adapted to values achieved by simulating the washing at approximately 10 000 different conditions. Only one parameter was varied each time in order to catch the interaction affects. A polynomial was fitted to the simulation data by using least square regression. The correlations are presented below.

$$SD_{in} = 0 \% \rightarrow SD_{out} = 272.51 * \Gamma^{-0.0775} + 600.32 * T^{0.0368} + 22.69 * L^{0.3972} - 975.25$$

$$SD_{in} = 31 \% \rightarrow SD_{out} = 103.10 * \Gamma^{-0.1408} + 1353.60 * T^{0.0134} + 12.93 * L^{0.4324} - 1504.82$$

$$SD_{in} = 63 \% \rightarrow SD_{out} = 36.32 * \Gamma^{-0.2182} + 1410.99 * T^{0.0092} + 5.89 * L^{0.4674} - 1441.56$$

The correlations are valid in the intervals 0.2-4 kg/ms, 40-100 ° C and 2-13 m. The mean accuracy for all three correlations is around 2 percentage points and the maximum deviation from the value predicted by the model is 12 percentage points of the saturation degree of the outgoing wash liquid.

8 Conclusions

An effective method to study and measure sodium scale dissolution rates in a falling film evaporator has been developed in this study. The dissolution rate was found to be proportional to the wetting degree. A higher wetting degree significantly increased the dissolution rate, but more wash liquid was required to dissolve the scaling layer. The washing behaviour also proved to be strongly dependent on the distribution of scales on the tube and on scales formed at other places than on the heat transfer surface. It was confirmed that the scaling layer grows from the bottom of the tube and upwards. Moreover, the scaling layer continues to grow until an equilibrium thickness is reached.

A mathematical model has been developed based on physical principles that successfully can predict the dissolution of sodium scales. The model was developed for the temperature interval 45-85 °C and wetting degrees of 0.13 kg/ms up to 0.44 kg/ms. The dissolution rate followed a first order expression with regards to the concentration difference between the scaling layer surface and the bulk of the wash liquid. The model was able to predict the outgoing salt concentration as well as the dissolution rate at two different positions on the tube, proving the validity of the model. The inconsistencies between the model and the observations were believed to be measurement errors.

To account for the temperature dependence of the transport coefficient k , a linear expression for k as a function of temperature was adapted using experimental data. When implementing the temperature dependent expression for k , a more accurate prediction was achieved for the experiments in which the wash temperature fluctuated. Furthermore, no dependence of wetting degree could be found for the transport coefficient k .

Correlations stating the outgoing saturation degree of the wash liquid as a function of wetting degree, temperature and length of the scaling layer at different ingoing saturation degrees were also developed. The correlations can successfully, with a mean error of 2 percentage points, estimate the saturation degree of the outgoing wash liquid in percentage. They are valid for water at wetting degrees between 0.2-4 kg/ms, temperatures of 40-100 °C and scaling layer lengths of 2-13 metres.

9 Further research

The pilot plant located at Chalmers is a great tool when exploring several topics regarding fouling and removal of scales. To simplify the experimental work and improve the accuracy of the results some improvements could be made to the pilot plant. To achieve a more accurate estimation of the scaling distribution, additional measurements between the two upper sight glasses are necessary. A method of how to accurately estimate the thickness from existing process data such as temperature differences from the thermocouples could also be of use. Furthermore, some uncertainties would be avoided if the ingoing wash liquid was connected directly to the flow distributor atop of the evaporator and the outgoing wash liquid was collected as it came off the tube. To enable a larger variety in washing temperature, the problem with insufficient cooling needs to be solved. An improvement could be to have a continuous flow of cooling water on the inside of the tube with the possibility to adjust the cooling water temperature in the range 20-90 °C. The problem with condensing vapour on the scaling layer will, however, remain.

To thoroughly investigate whether the mass transport coefficient is dependent on wetting degree or not, experiments at higher wetting degrees should be conducted. To enable a higher flow, existing piping in bottom of the evaporator has to be replaced. It would also be interesting with lower wetting degrees than used in this study, but there is a problem with insufficient wetting of the tube that has to be solved.

Further work is needed to investigate whether the dissolution process is dependent on viscosity and pH, two important properties of black liquor. Industry often use diluted weak black liquor a wash liquid, which has a significantly higher viscosity and pH compared to deionised water. The higher viscosity will influence the flow properties and more specifically result in a wavy laminar film. Thus, efforts should be made to investigate how the mass transport is affected by a more laminar bulk flow. A higher pH can shift the equilibrium reactions and thus have an impact on the solubility of the salts. Weak black liquor deviates from deionised water in several other ways than viscosity and pH, especially its complex composition might have a strong effect on the dissolution rate. A model valid for different wash liquids should therefore be developed. Furthermore, to fully investigate and model the dissolution rate the type of scales covering the tube should be varied, i.e. whether burkeite, dicarbonate or carbonate have crystallised.

Scaling in black liquor evaporators is not only caused by sodium salts, but several substances are involved. The scaling layer in black liquor evaporators might thus have different dissolution behaviour compared to those originating entirely from a sodium salt solution. The dissolution process of a scaling layer formed during evaporation of black liquor is therefore an important area to explore.

Finally, the proposed mathematical model can be implemented in several ways beside the correlation developed in this study. More work is needed in this area to develop general and specific guidelines regarding washing procedures in industry.

References

- Axelsson, E., Olsson, M.R. & Berntsson, T., 2006. Heat integration opportunities in average Scandinavian kraft pulp mills□: Pinch analyses of model mills. *Nordic Pulp and Paper Research Journal*, 21(4), pp.466–475.
- Bird, R.B., Stewart, W.E. & Lightfoot, E.N., 1960. *Transport phenomena*, New York: John Wiley & Sons, Inc.
- Brännvall, E. et al., 2008. *The Ljungberg Textbook - Cellulose Technology*, Stockholm: Forest Products and Chemical Engineering, Dept. of Chemical and Biological Engineering, Chalmers University of Technology.
- Changani, S.D., Belmar-Beiny, M.T. & Fryer, P.J., 1997. Engineering and chemical factors associated with fouling and cleaning in milk processing. *Experimental Thermal and Fluid Science*, 14(4), pp.392–406.
- Chen, F.C. & Gao, Z., 2004. An analysis of black liquor falling film evaporation. *International Journal of Heat and Mass Transfer*, 47(8-9), pp.1657–1671.
- Clay, D.T., 2008. Evaporator fouling.
- Costa, A. et al., 2007. Economics of trigeneration in a kraft pulp mill for enhanced energy efficiency and reduced GHG emissions. *Energy*, 32(4), pp.474–481.
- Dokoumetzidis, A. & Macheras, P., 2006. A century of dissolution research: from Noyes and Whitney to the biopharmaceutics classification system. *International journal of pharmaceutics*, 321(1-2), pp.1–11.
- Eneberg, H., Kaila, J. & Kiiskila, E., 2000. Method of inhibiting scaling in black liquor evaporators.
- Engman, W.C. & Clark, W.W., 1970. Removing and inhibiting scale in black liquor evaporators.
- Euhus, D. et al., 2003. Eliminating sodium salt fouling in black liquor concentrators: Crystallization behavior and fouling in pilot evaporation trials. In *Fall Technical Conference*.
- Euhus, D., 2003. *Nucleation in bulk solutions and crystal growth on heat transfer surfaces during evaporative crystallization of salts composed of Na₂CO₃ and Na₂SO₄*. Georgia Institute of Technology.
- Frederick, Shi, B. & Euhus, D., 2004. Crystallization and control of sodium salt scales in black liquor concentrators. *Tappi Journal*, 3(6), pp.7–13.
- Frederick, Verrill, C.L. & Rousseau, R.W., 2004a. Controlling Sodium Salt Deposits in Black Liquor Evaporators□: A Review. In *TAPPI International Chemical Recovery Conference*. Charleston.

- Frederick, Verrill, C.L. & Rousseau, R.W., 2004b. High Performance Evaporators: A Summary of Findings, Potential Applications, and Research Needs to Reduce or Eliminate Soluble Scale Fouling in High-Solids Black Liquor Concentrators. *TAPPI Paper Summit - Spring Technical and International Environmental Conference. International Environmental Conference.*
- Frederick, W.J., Verrill, C.L. & Rousseau, R.W., 2004c. Controlling Sodium Salt Deposits in Black Liquor Evaporators □: A Review. In *TAPPI International Chemical Recovery Conference*. Charleston.
- Gill, J.S. & Henderson, K.F., 1995. Controlling scale in black liquor evaporators.
- Gourdon, M., 2009. *Sodium Salt Scaling in Black Liquor Evaporators*. Chalmers University of Technology.
- Gourdon, M., Olausson, L. & Vamling, L., 2011. Evaporation of Na₂CO₃-Na₂SO₄ solutions: A method to evaluate the distribution between bulk and surface crystallization. *Tappi Journal*, (March), pp.17–24.
- Grant, C.S., Perka, A.T., et al., 1996. Cleaning of solid behenic acid residue from stainless-steel surfaces. *AIChE Journal*, 42(5), pp.1465–1476.
- Grant, C.S., Webb, G.E. & Jeon, Y.W., 1996. A noninvasive study of milk cleaning processes: calcium phosphate removal. *Journal of Food Process Engineering*, 20(1997), pp.197–230.
- Haag, J. & Stigson, S., 2003. *Lutlagring och lutföringens inverkan på inkrustering i indunstningsapparater och cisterner*, Stockholm.
- Jennings, W.G., 1959. Circulation Cleaning. III. The Kinetics of a Simple Detergent System. *Journal of Dairy Science*, 42(11), pp.1763–1771.
- Kern, D.Q. & Seaton, R.E., 1959. A theoretical analysis of thermal surface fouling. *British Chemical Engineering*, 12, pp.258–262.
- Konopa, J., 1997. Multiple effect evaporator throughput extension with unique chemistry. *Paper Age*.
- Kramers, H. & Kreyger, P.J., 1956. Mass transfer between a flat surface and a falling liquid film. *Chemical Engineering Science*, 6, pp.42–48.
- MacAdam, J. & Parsons, S.A., 2004. Calcium carbonate scale formation and control. *Reviews in Environmental Science and Biotechnology*, 3(2), pp.159–169.
- Mateos-Espejel, E. et al., 2010. Systems interactions analysis for the energy efficiency improvement of a Kraft process. *Energy*, 35(12), pp.5132–5142.
- Murray, A.P., 1987. Modeling nuclear decontamination processes. *Nuclear technology*, 77(2), pp.194–209.

- Müller-Steinhagen, Z., 1997. Heat transfer and heat transfer fouling in Kraft black liquor evaporators. *Experimental Thermal and Fluid Science*, 14(4), pp.425–437.
- Nernst, W. & Brunner, E., 1904. Theorie der Reaktionsgeschwindigkeit in heterogenen systemen. *Zeitschrift für Physikalische Chemie*, 47, pp.57–102.
- Noyes, A. & Whitney, W., 1897. The rate of solution of solid substances in their own solutions. *Journal of the American Chemical Society*, 19(12), pp.930–934.
- Schmidl, W. & Frederick, 1998. Current trends in evaporator fouling. In *International Chemical Recovery Conference*. Tampa, Florida, pp. 367–377.
- Schnabel, G., 1988. *VDI-Wärmeatlas □: Berechnungsblätter für den Wärmeübergang / Herausgeber Verein Deutscher Ingenieure* 5th ed., Düsseldorf: VDI-Verlag GmbH.
- Shi, B., 2002. *Crystallization of solutes that lead to scale formation in black liquor evaporation*. Georgia Institute of Technology.
- Skogsindustrierna, 2010. Skogsindustrin - En faktasamling, 2010 års branschstatistik.
- Verrill, C.L. & Frederick, 2005. *Evaporator Fouling 101 - Sodium Salt Crystallization and Soluble-scale Fouling*, Atlanta: Georgia Institute of Technology.
- Welty, J.R. et al., 2008. *Fundamentals of Momentum, Heat, and Mass Transfer* 5th ed., John Wiley & Sons, Inc.

Appendix

1. Volume expansion factor

A correlation between density and the content of dry substance for a sodium, sulphate and carbonate solution has been developed. The correlation was derived by rewriting the definition for both density and dry substance measurements in the following way.

The density of the solution can be expressed as:

$$\rho_{solution} = \frac{m_{solution}}{V_{solution}}$$

And therefore the mass of the solution can be expressed as:

$$\Rightarrow m_{solution} = \rho_{solution} * V_{solution}$$

Dry substance measurement of a solution is calculated as:

$$TS = \frac{m_{salt}}{m_{salt} + m_{water}} = \frac{m_{salt}}{m_{solution}} = \frac{m_{salt}}{\rho_{solution} * V_{solution}}$$

The weight of the salt can then be rewritten as:

$$m_{salt} = m_{solution} - m_{water} = \rho_{solution} * V_{solution} - \rho_{water} * V_{water}$$

This will result in the following expression for dry substance measurement:

$$\begin{aligned} \Rightarrow TS &= \frac{\rho_{solution} * V_{solution} - \rho_{water} * V_{water}}{\rho_{solution} * V_{solution}} \\ \Rightarrow TS &= 1 - \frac{\rho_{water} * V_{water}}{\rho_{solution} * V_{solution}} \end{aligned}$$

In this expression everything is known except the volume of the water and the volume of the solution. Let us however assume that there exist some sort of function that dependent on a specific salt concentration can estimate how much bigger the solution volume is in comparison to water. Then the expression could be simplified into this.

$$\begin{aligned} V_{solution} &= V_{water} * f \\ \Rightarrow TS &= 1 - \frac{\rho_{water} * V_{water}}{\rho_{solution} * V_{water} * f} \\ \Rightarrow TS &= 1 - \frac{\rho_{water}(T_{out})}{\rho_{solution}(T_{out}) * f(TS)} \end{aligned}$$

The function f was calculated based on measurements on containers with different salt content. The containers were heated to different temperature to make sure that the developed function was temperature independent, which was the case.

The function turned out to be a third degree polynomial on the following form.

$$f(TS) = 0.8341 * (TS)^3 + 0.5579 * (TS)^2 + 0.0267 * (TS) + 1$$

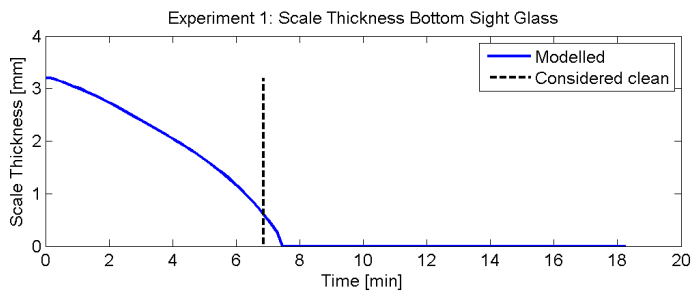
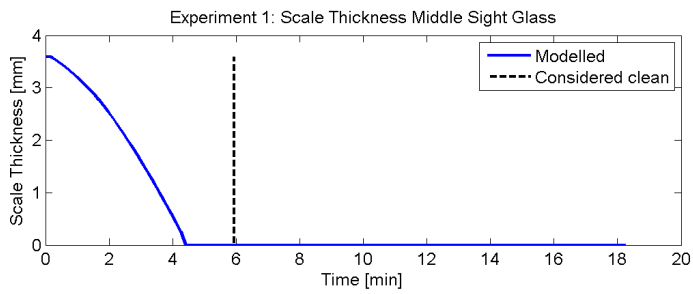
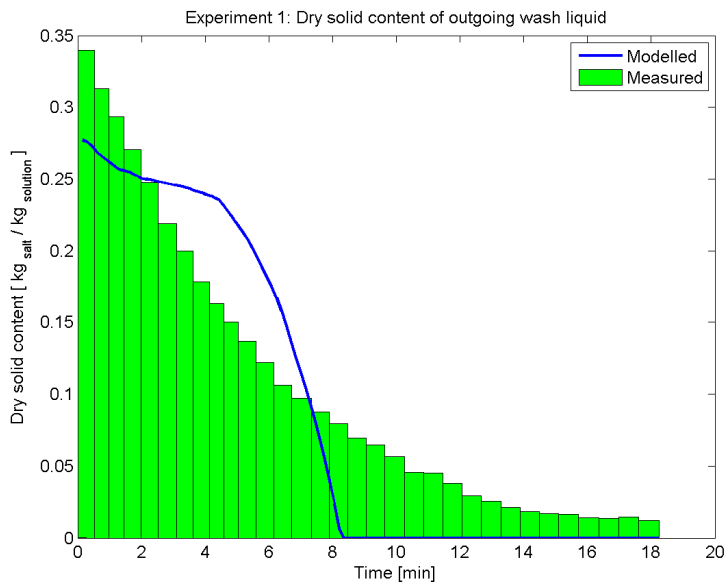
The function could then be used together with the above equation to iteratively calculate the dry substance of the solution as long as density and temperature is known.

2. Experimental data

Experimental conditions, together with wash curves and the 1st order model with the adapted linear temperature dependence for all eight performed experiments are presented below. How well the 1st order model can predict the dissolution rate at the middle and bottom sight glasses can also be seen. In experiment 1-4 the model accuracy is compared with data obtained from the video cameras regarding when the tube was considered clean. In experiments 5-8, a measurement device had been installed so the model is compared against several measurements of the thickness of the scaling layer during washing.

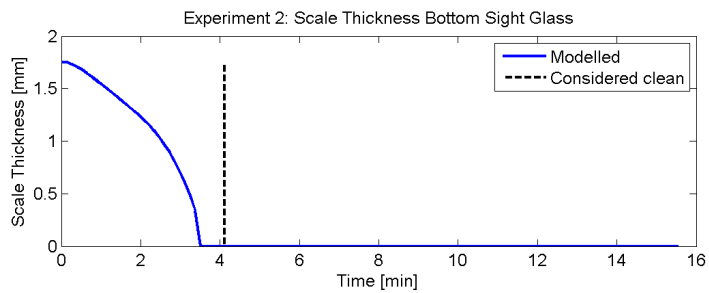
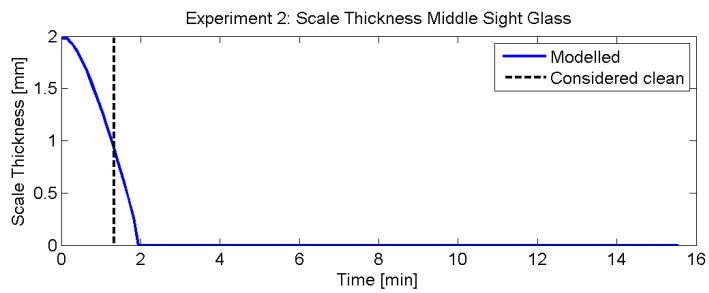
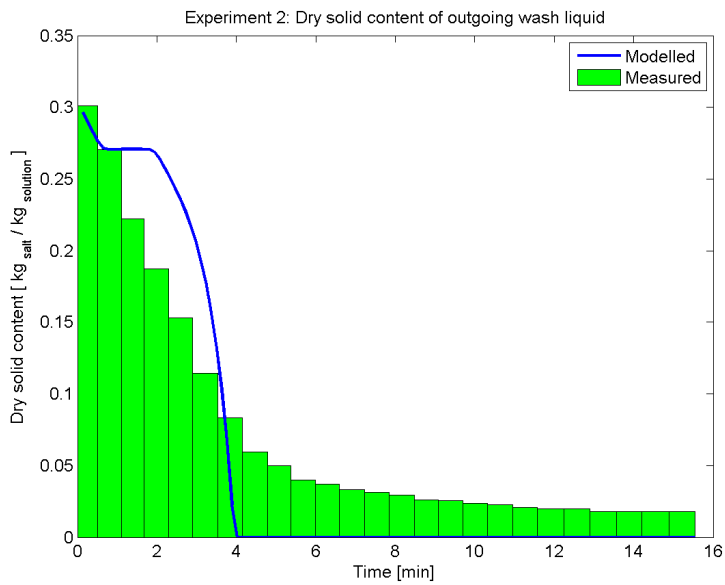
Experiment 1

Experimental parameters	Value	Unit
Wetting degree	0.157	kg/ms
Temperature in	40 °C	°C
Mean temperature out	52 °C	°C
Salt on the tube	4.0 kg	kg
Wash liquid required	24	l



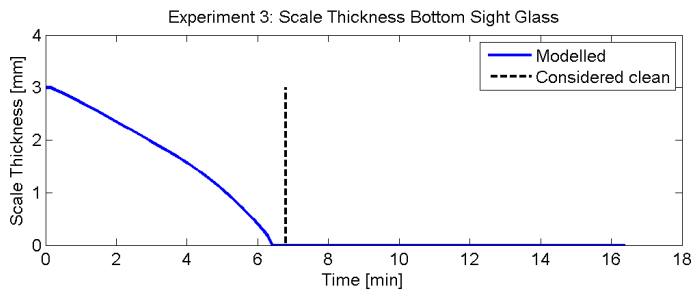
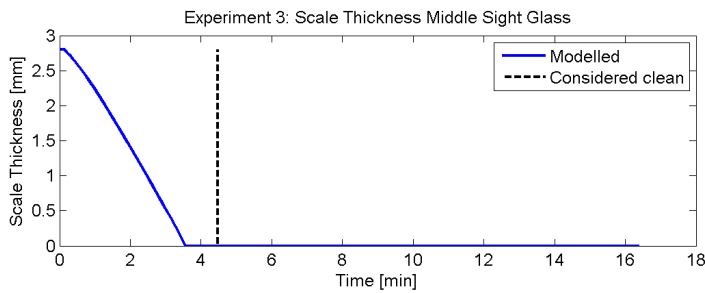
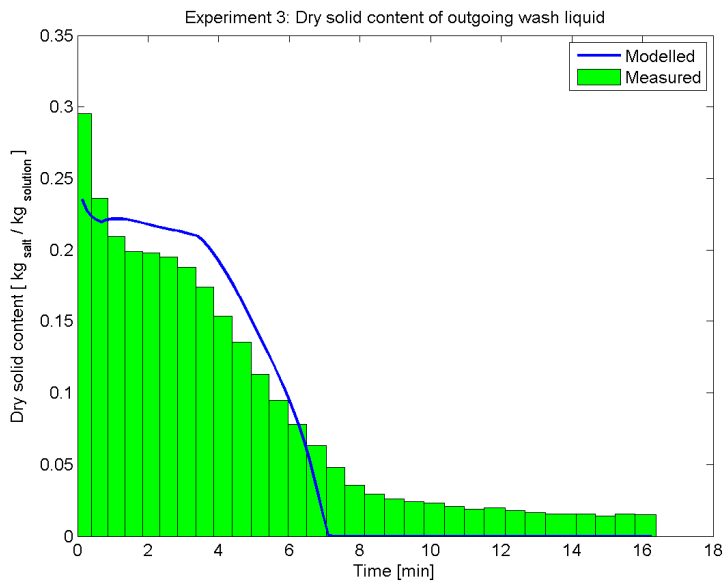
Experiment 2

Experimental parameters	Values	Unit
Wetting degree	0.139	kg/ms
Temperature in	76	°C
Mean temperature out	76	°C
Salt on the tube	1.8	kg
Wash liquid required	10	l



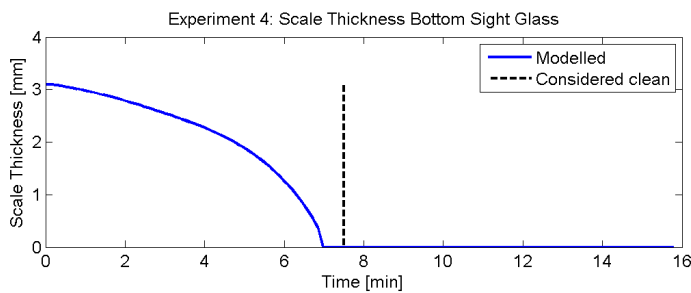
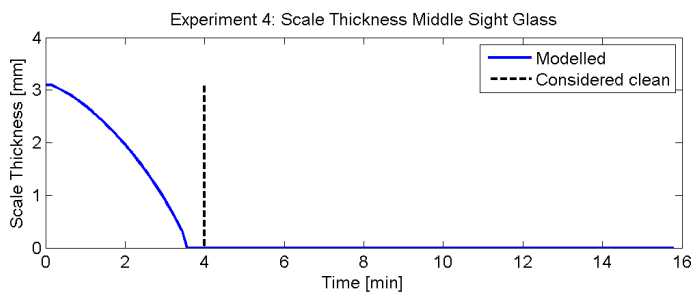
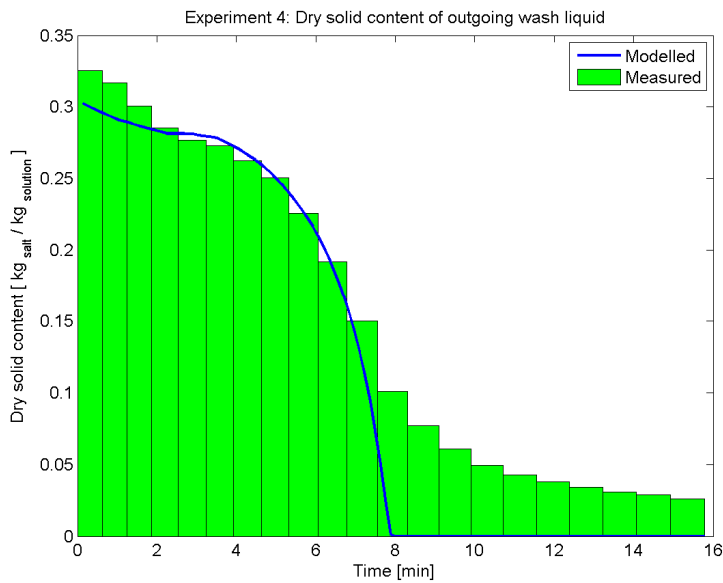
Experiment 3

Experimental parameters	Values	Unit
Wetting degree	0.168	kg/ms
Temperature in	45	°C
Mean temperature out	48	°C
Salt on the tube	2.9	kg
Wash liquid required	17	l



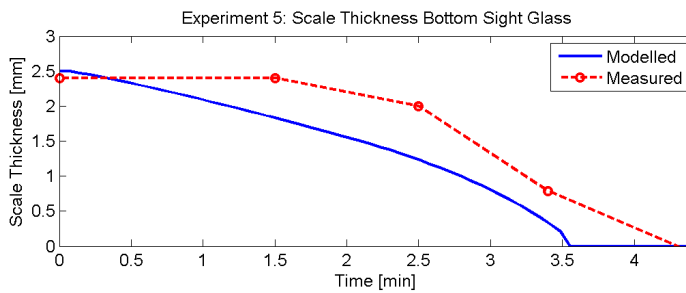
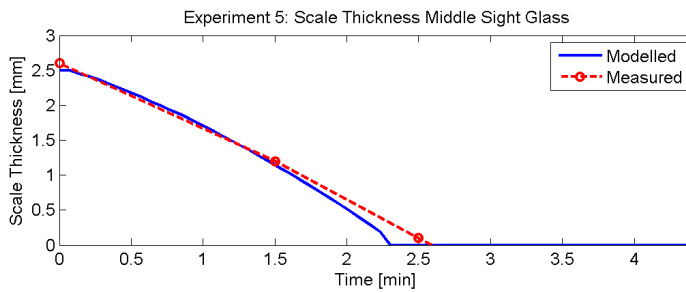
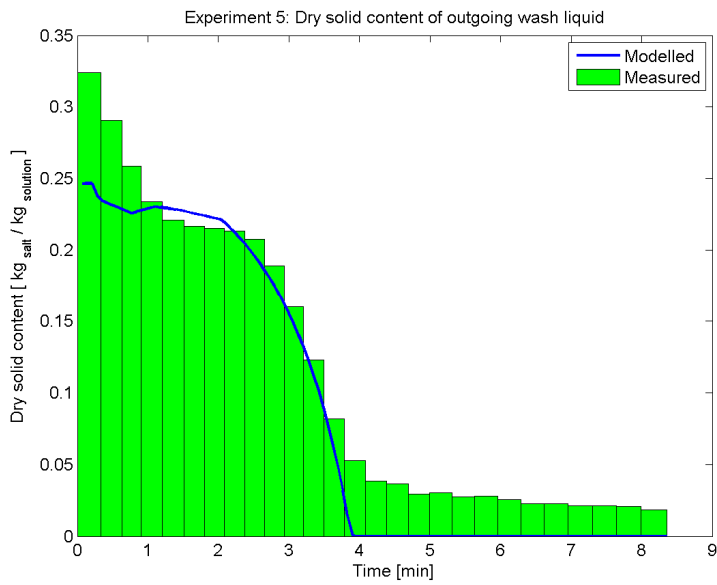
Experiment 4

Experimental parameters	Values	Unit
Wetting degree	0.123	kg/ms
Temperature in	84	°C
Mean temperature out	81	°C
Salt on the tube	3.9	kg
Wash liquid required	16	l



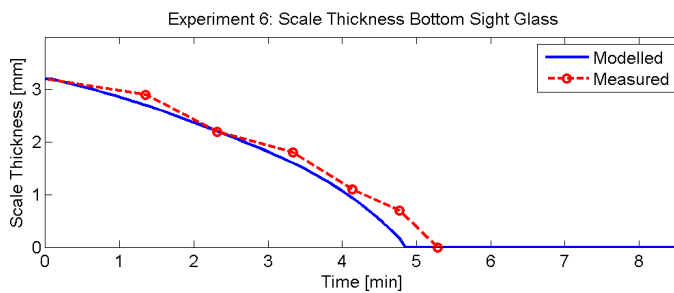
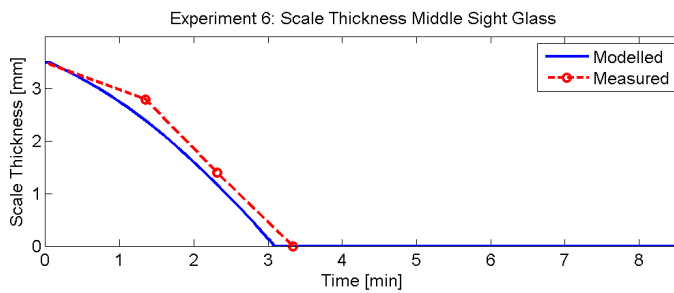
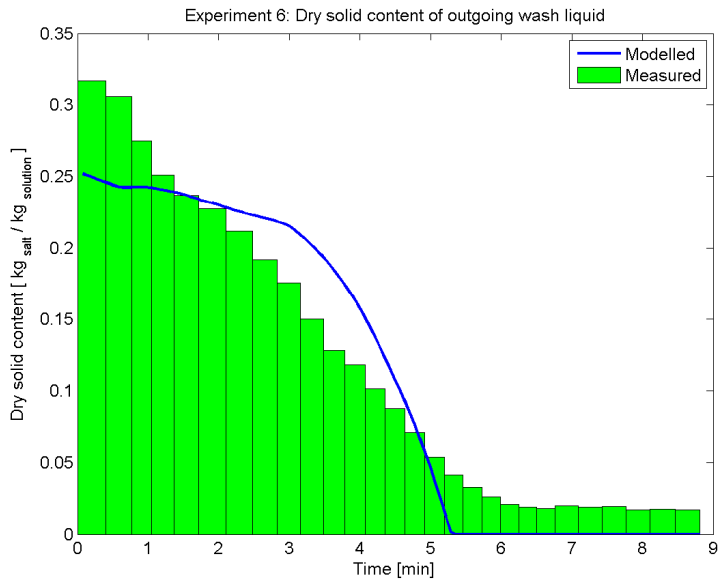
Experiment 5

Experimental parameters	Values	Unit
Wetting degree	0.295	kg/ms
Temperature in	82	°C
Mean temperature out	78	°C
Salt on the tube	3.8	kg
Wash liquid required	19	l



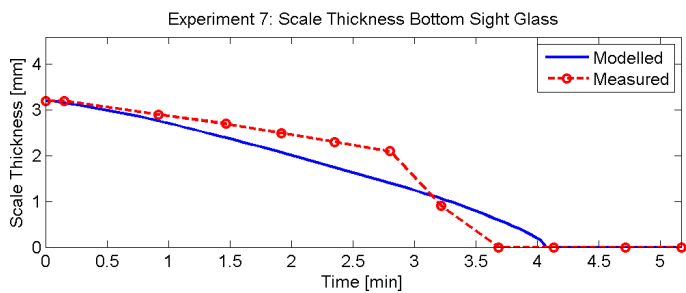
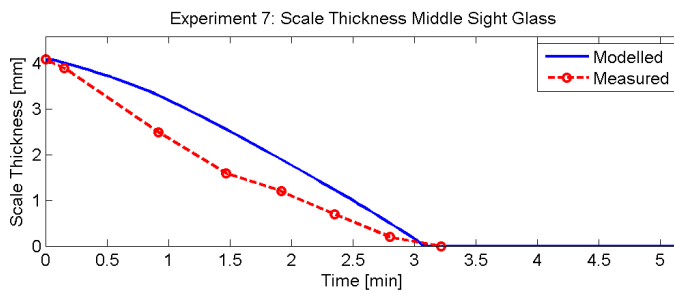
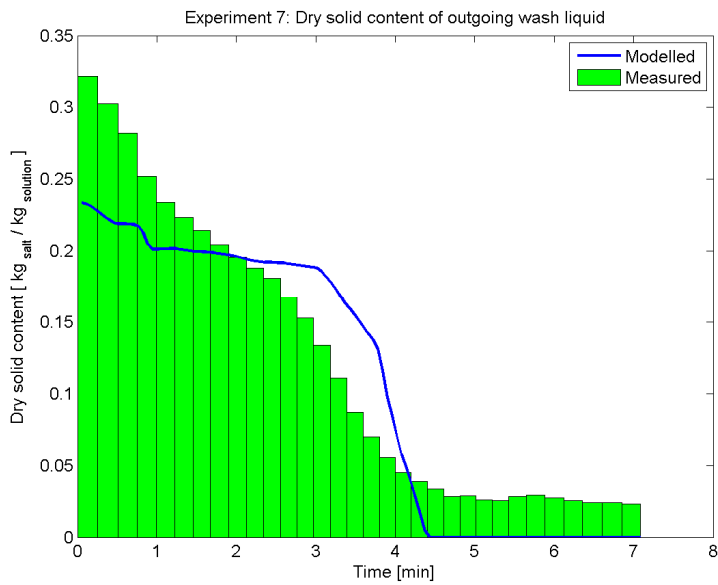
Experiment 6

Experimental parameters	Values	Unit
Wetting degree	0.287	kg/ms
Temperature in	63	°C
Mean temperature out	75	°C
Salt on the tube	3.8	kg
Wash liquid required	21	l



Experiment 7

Experimental parameters	Values	Unit
Wetting degree	0.401	kg/ms
Temperature in	84	°C
Mean temperature out	84	°C
Salt on the tube	4.4	kg
Wash liquid required	22	l



Experiment 8

Experimental parameters	Values	Unit
Wetting degree	0.432	kg/ms
Temperature in	63	°C
Mean temperature out	72	°C
Salt on the tube	4.1	kg
Wash liquid required	24	l

